

33

Abstract

34 Large-scale palaeoclimate reconstructions can be very sensitive to the proxy records they are based
35 on, and hence to the criteria used to select proxy records. Data selection rarely follows objective
36 criteria that are applicable to all types of proxies, including both low- and high-resolution records. Thus,
37 there is a need for a uniform and transparent approach to assess the suitability of input proxy data for
38 a reconstruction. Here, we develop classification criteria that are applicable to multiple proxy types
39 and evaluate different selection strategies using a network of 62 millennium-long terrestrial
40 hydroclimate proxy records from Monsoon Asia. Our results reveal that robust evidence for a coherent
41 climate signal and high dating accuracy are important criteria for benchmarking the suitability of each
42 proxy record. We determine these criteria by reviewing the literature for each record (rather than
43 screening against instrumental data). We show that the proposed selection approach can yield a
44 network with a stronger common signal. By evaluating the uncertainty and centennial variability of
45 composite reconstructions, from differently selected subsets of the proxy network, it appears
46 beneficial to use suitable proxies stemming from different archives, as well as having a dense network
47 of proxy sites. We suggest that future large-scale palaeoclimate reconstructions might be improved by
48 evaluating proxy networks according to the universal categories presented here and, if indicated,
49 removing less suitable records. This will strengthen the climate signal in the final reconstruction,
50 allowing more precise inferences about past climate variability and more robust comparisons with
51 climate model simulations.

52

53

Keywords

54 Holocene; Paleoclimatology; Eastern Asia; Data treatment; Large-scale reconstruction; Low resolution;
55 Expert assessment; Spatial decorrelation length; Multi-proxy

56

57 **1. Introduction**

58 Our ability to reconstruct the Earth's climatic history and assess the impacts of past climate changes
59 on human history is dependent on identifying and interpreting archives of past climate variability (e.g.
60 Masson-Delmotte et al., 2013; Xoplaki et al., 2016; Ljungqvist, 2017; Xoplaki et al., 2018). The field of
61 palaeoclimatology has advanced over the past decade through the increase of the spatial coverage
62 and density of temperature and hydroclimate proxy records on a regional basis, the development of
63 new multi-proxy reconstruction methodologies as well as the increasing number of quantitative
64 palaeoclimate reconstructions covering the past one to two millennia (Christiansen and Ljungqvist,
65 2012; Ljungqvist et al., 2012; PAGES2k Consortium, 2013; Neukom et al., 2014; Schneider et al., 2015;
66 Stoffel et al., 2015; Ljungqvist et al., 2016; Luterbacher et al., 2016; Wilson et al., 2016; Xing et al.,
67 2016; PAGES2k Consortium, 2017). With the growing proxy network, significantly different evaluations
68 of past climates can be obtained, depending on individual choices during the proxy selection step
69 (Frank et al., 2010; Smerdon and Pollack, 2016; Christiansen and Ljungqvist, 2017). Despite a common
70 spatial target, authors may impose criteria constraining the number of proxy records by requiring a
71 minimum temporal length and resolution of proxy time-series (Schneider et al., 2015; PAGES2k
72 Consortium, 2017; Esper et al., 2018). Focusing only on a single proxy type can increase homogeneity
73 among records. At the same time, it can accentuate limitations associated with this proxy type and
74 further confine the size of the proxy network. For investigations on hemispheric to global scales, these
75 selection strategies can alter the number of eligible proxy records from below 20 (Schneider et al.,
76 2015) to almost 700 (PAGES2k Consortium, 2013, 2017) to include in large-scale temperature
77 reconstructions.

78 The difference in the size of proxy networks raises the question whether there is a threshold beyond
79 which the addition of more, but noisier, records is not useful anymore. To answer this question, the
80 strengths and weaknesses of individual records need to be communicated clearly in order to facilitate
81 the selection of palaeoclimate data (Frank et al., 2010; Esper et al., 2016; Christiansen and Ljungqvist,
82 2017; Esper et al., 2018). Defining objective and universal measures for this purpose is nontrivial.

83 Large-scale reconstructions often include a screening (e.g. Zhang et al., 2018) and/or weighting (e.g.
84 Cook et al., 2002; Pauling et al., 2003; Luterbacher et al., 2004; Xoplaki et al. 2005; Luterbacher et al.,
85 2016; Wang et al., 2017) of records based on the correlation between proxy and instrumental
86 observations. Although this is arguably the most objective measure it also bears a number of
87 shortcomings. First, the climate signal strength often cannot be determined conclusively, due to short
88 instrumental data, meteorological information that is remote from the proxy location or lower quality
89 of early measurements (Parker, 1994; Moberg et al., 2003; Frank et al., 2007; Dienst et al., 2017).
90 Second, the proxy data often have a limited temporal resolution and terminate in the year of sampling
91 further reducing the degrees of freedom in any calibration approach (e.g. Yao et al., 1996). Third, the
92 quality of the proxy record can change over time. This can be due to changing temporal resolution,
93 increasing age uncertainty (Kaspari et al., 2007; Kuo et al., 2011) or human impact (Liu et al, 2008).
94 Tree-ring records usually have a decreasing replication back in time and thus an increasing uncertainty
95 (Esper et al., 2007; Esper and Frank, 2009; Esper et al., 2016). Likewise, the spatial coverage for
96 documentary data gets sparser in the more distant past (Brázdil et al., 2005, 2018).

97 The choice of only annually dated proxy records will resolve some of these problems and would, in
98 principle, allow for a relatively robust screening, but with the price of reducing the number of available
99 proxy records further back in time (e.g. Luterbacher et al., 2016; Zhang et al., 2018). Moreover,
100 instrumental data from some regions are much shorter than 100 years. For example, observations at
101 most sites on the Tibetan Plateau did not start before 1950 CE (e.g. Duan et al., 2017). Successful
102 calibration with a short overlapping period depends strongly on the high frequency signal. At these
103 frequencies, annually resolved documentary records and tree-ring chronologies often have a high
104 fidelity while multi-centennial or millennial variability can be underestimated due to discontinuity of
105 data sources (Cook et al., 1995; Brázdil et al., 2005; Dobrovolný et al., 2010; Wetter and Pfister, 2011;
106 Brázdil et al., 2018; Pfister et al., 2018). Although there are different methods to consider or moderate
107 this bias (Esper et al., 2003; Melvin and Briffa, 2008; Glaser and Riemann, 2009), it remains difficult to
108 quantify the extent to which low-frequency variability may be lacking in these records. The

109 combination with records from continuous archives, but with lower temporal resolution (from lake
110 and marine sediments, peat bogs or speleothems), can help to overcome deficits in the low frequency
111 domain while impeding calibration and validation. Additionally, blending annually resolved time-series
112 with records of lower resolution can improve spatial coverage, which is of particular concern for
113 studies targeting hydroclimate (Smerdon et al., 2017). Compared to temperature, precipitation and
114 drought are much more variable across space (Büntgen et al., 2010; Cook et al., 2010), in particular
115 over complex terrain (Feng et al., 2013), and have much shorter correlation decay lengths (Datta et al.,
116 2003; Wan et al., 2013; Ljungqvist et al., 2016). This requires a denser proxy network in combination
117 with a smaller search radius for meteorological stations with long observational time-series.
118 Consequently, there may be less confidence regarding past hydroclimate variability in space and time
119 than for temperature (Büntgen et al., 2010; Bunde et al., 2013; Franke et al., 2013; Masson-Delmotte
120 et al., 2013; Ljungqvist et al., 2016; Smerdon et al., 2017).

121 In this study, we address the challenge of proxy selection and evaluation in a region rich in
122 documentary and natural proxy records, but with short instrumental data: Monsoon Asia. We analyze
123 hydroclimate variability as the most relevant parameter from a societal perspective in this part of the
124 world and target the entire last millennium (1000–1999 CE). Precipitation and drought variability have
125 been investigated across Eastern Asia for the 1300 - 2000 CE period using the region's dense network
126 of tree-ring chronologies and documentary records (Cook et al., 2010; Feng et al., 2013; Zhang et al.
127 2015; Shi et al., 2017, 2018). Extending a spatial field reconstruction before 1300 CE will require the
128 inclusion of additional archives and proxy types to maintain a full spatial coverage. Rather than
129 presenting a new quantitative hydroclimate reconstruction, we use alternative proxy selection
130 strategies to filter the noisy network and to evaluate the impact of the proxy network's composition.
131 Our approach overcomes the limitations of a screening based on instrumental data while relying on a
132 combination of metadata analysis and the "expert assessment" of the original authors (Frank et al.,
133 2010; Wilson et al., 2016; Christiansen and Ljungqvist, 2017). The 62 hydroclimate records used in this
134 study stem from lake sediments, speleothems, historical documentary data, tree-rings and ice-cores

135 (Fig. 1). The variety of archives and proxy types introduces significant differences among individual
136 records regarding the evolution and the characteristics of time-series, which are most likely not only
137 driven by regional hydroclimatic changes, but also indicate varying levels of precision. We hypothesize
138 that the common signal will be stronger among more suitable records than among less suitable ones,
139 and that careful scrutiny and selection of the proxy records based on metadata will, therefore, yield a
140 more robust reconstruction. In order to test this hypothesis, we define suitability measures that can
141 be derived from the individual source publications. We emphasize the reproducibility of the procedure
142 by using criteria that can be transferred to a wide range of palaeoclimate records. We evaluate the
143 reliability of the resulting classification and assess its impact for subsequent proxy selection on regional
144 means. We close by suggesting that the choice between a comprehensive or a selective proxy network
145 should be based on transparent and measurable characteristics.

146

147 **2. Data and Methods**

148 The proxy records analyzed in this study (Fig. 1, Table 1) have been published in the peer-reviewed
149 literature. If possible the data for the 62 records were obtained from online repositories or, if
150 unavailable, via personal communication with authors and data contributors. All records were
151 originally described as indicative of local variations in hydroclimate. The term hydroclimate
152 incorporates variations in precipitation, moisture, streamflow or drought. Although some of these
153 parameters integrate temperature conditions as well, this generalization was necessary to warrant a
154 sufficiently large network. The region spans 20-50°N and 70-130°E (Fig. 1), which includes areas
155 impacted by the Indian Summer Monsoon, the East Asian Summer Monsoon and the Westerlies that
156 interact with the northern monsoon limit. To preserve multi-decadal to multi-centennial variability
157 during the last millennium, we retrieved only data matching the following criteria: a start date of proxy
158 records before 1001 CE, a minimum temporal resolution of 50 years (at least two data points per
159 century) and one fixed dating point in the last millennium (compare Ljungqvist et al., 2016). The final
160 network consists of 17 lake sediment (excluding pollen), 14 documentary, 13 speleothem, nine tree-

161 ring (including two reconstructions based on tree-ring isotopes), 7 pollen¹ and 2 ice-core records (Fig.
162 1, Table 1). The proxy types are not homogeneously distributed over the study area. Eastern China is
163 rich in documentary data (e.g. Ge et al., 2008) while moisture sensitive tree-ring records are numerous
164 over the northern fringe of the Tibetan Plateau, where slow growth enables trees to grow particularly
165 old (Yang et al., 2014a). Lake sediments are least regionally confined and can be found all over the
166 study region. With 15 different analyzed parameters – e.g. grainsize (Conroy et al., 2017), CaCO₃
167 content (Li et al., 2004), total organic carbon amount (Xiao et al., 2008) – lake sediments reveal the
168 greatest variety of proxy types within a specific archive.

169 While the initial selection criteria mentioned above ensure a minimum amount of common climate
170 information in the proxy records, a further screening based on their correlation with local observations
171 is not possible in most cases. Only 10 out of 62 records (two documentary, two speleothems and six
172 tree-ring chronologies) have annual resolution; 40 records have two or less data points per decade.
173 This results in – at best – about 10 degrees of freedom for calibrating records from the Himalayas, the
174 Tibetan Plateau and northwestern China where very few stations were running before the 1950s (Cook
175 et al., 2010; Krusic et al., 2015). In Eastern China, where many instrumental records are longer, the
176 majority of proxy records are based on documentary data. For this archive, a screening is challenging
177 because historical observations were usually replaced by measurements from meteorological stations
178 after their start during the course of the 20th century. Thus, documentary datasets are often
179 complemented using instrumental observations (e.g. Zheng et al., 2006; Zhang et al., 2008) making it
180 impossible to evaluate these data based on the instrumental overlap.

181 Not all of the 62 records are similarly suitable for reconstructing hydroclimate over the last millennium
182 because the various studies address very different frequency domains from multi-millennial to multi-

¹ Pollen records are usually derived from lake sediments. However, we chose to separate pollen records here, because they represent a large and important group of parameters that can be measured in lake sediments. This classification is in accordance with the one used by NOAA's National Centers for Environmental Information database.

183 decadal. We acknowledge that all records might be skillful predictors regarding their originally targeted
184 time scale and, therefore, we use the term “suitability” as a measure of relevance for each record in
185 our context. To assess the suitability while avoiding calibration with instrumental data, we defined two
186 categories that address: (1) the dating accuracy (DA), and (2) the evidence for a climate signal (EC) in
187 the original publications. As both measures cannot be directly quantified, we use an ordinal scale with
188 three classes for each category.

189 (1) The DA is “good” (+1) for documentary records and for natural archives with visually
190 discernible annual layers. Records of “intermediate” (0) DA either offer layer counting or a
191 comprehensive age model that has 5 or more dating points in the correct chronological order
192 (within uncertainties) during the past millennium. “Insufficiently” (-1) dated records do not
193 fulfill these requirements. The estimate is based on the longer sequence, if DA changed within
194 the last millennium, for example due to the fading of laminae (e.g. Paulsen et al., 2003).

195 (2) There is “good” (+1) EC in the proxy record if the source publication contains a robust
196 calibration against instrumental data. If the temporal resolution is low and/or the instrumental
197 record short, the climatic sensitivity of the proxy needs instead to be described theoretically –
198 ideally confirmed by a monitoring experiment. If the authors present a mechanistic
199 understanding of the relationship between proxy and climate and if the time-series is
200 evaluated with respect to other climate reconstructions from the same region, we grade this
201 as an “intermediate” (0) EC. Studies that only address one of these lines of argument have
202 “insufficient” (-1) EC.

203 Although a “good” EC again requires a comparison with instrumental data, the category is different
204 from regular quantitative screening approaches in large-scale network evaluations. Longer and/or
205 closer station measurements might have been available to the original authors to verify a climate
206 signal, whereas a standardized computation of correlations with interpolated and infilled observations
207 is more prone to biases.

208 Time-series with irregularly spaced time-steps need an adjustment to a common time-scale for
209 comparisons. Following the approach of Ljungqvist et al. (2016), records were linearly interpolated to
210 annual resolution. For the analysis of centennial to millennial scale climate signals, records were low-
211 pass filtered with a 100-year cubic spline and a 50 percent frequency cutoff (Cook and Peters, 1981;
212 Bunn, 2010). Climate signals in the range of decades were emphasized by subtracting the low-pass
213 filtered series from the original records and smoothing the remainder with a 20-year spline and 50
214 percent frequency cutoff. These low- and band-pass filtered time-series with annual time-steps were
215 normalized with respect to the common 1000–1900 CE period and subsequently subsampled in 10-
216 and 50-years intervals to account for the fact that most of the original records were not annually
217 resolved. Subsequent analyses were performed separately with time-series of 10- and 50-years
218 resolution to better capture time-scale dependent behavior (Fig. 2 and 3).

219 Initial approaches to evaluate the proxy records and their categorization using gridded climate data,
220 such as CRU TS3.10 (Harris et al., 2014) and the Twentieth Century Reanalysis (20CR) (Compo et al.,
221 2011; Slivinski et al., 2019), failed due to insufficient data overlap. Instead, we use an existing 530-year
222 climate reconstruction for China (Shi et al., 2017; henceforth Shi17). The precipitation reconstruction
223 is based on a dense set of 491 tree-ring and 108 documentary records and shows good verification
224 skills over large parts of China. Most of the Shi17 documentary records belong to a 530-year long
225 structured compilation of data from 120 subregions that cover Eastern China (Academy of
226 Meteorological Science, 1981). The Shi17 tree-ring sites are predominantly located on the Tibetan
227 Plateau or the surrounding highlands. The tree-ring chronologies are of variable length, but mostly
228 shorter than 530 years, so that the reconstruction quality most likely decreases back in time. The Shi17
229 data also include millennial-long records that overlap with the dataset analyzed herein (Fig. 2). Hence,
230 the majority of tree-ring and documentary records used in this study cannot act as fully independent
231 samples. The correlation between Shi17 and the proxy network was calculated between each proxy
232 site and the closest grid point of the precipitation reconstruction.

233 A Spearman rank-difference correlation between each proxy record and an average of its six closest
234 neighbors yields estimates of the coherency within the proxy network and of the spatial correlation
235 decay length (Fig. 3). Although Pearson correlations between hydrological parameters are expected to
236 yield similar results (McDonald and Green, 1960), we used the Spearman correlation to account for
237 the fact that it is more robust against outliers observed in the proxy data. The number of neighbors
238 considered was optimized in order to maximize the mean of all correlations. Tests with five or less
239 neighbors resulted on average in lower correlations presumably because of a less effective noise
240 cancelation in the neighbors average. More than six neighbors required an increased search radius.
241 Considering more distant sites for the neighbors average likewise decreased correlations overall.
242 Neighbors were chosen independent of the proxy type. Considering only records with good DA and EC
243 as neighbors also increased the average distance of neighbors and, more importantly, reasoning will
244 be circular because we aim at testing the DA- and EC-classification using the resulting coherency
245 estimates.

246 Chen et al. (2015b) show that our study area can be divided in 3 clusters with different evolutions of
247 hydroclimate over the past millennium. Guided by these clusters and with a focus on regions with the
248 densest proxy coverage (northeastern Tibetan Plateau and Eastern China), we subdivided our region
249 into three subregions (Fig. 1) that are expected to have a similar hydroclimate history (Chen et al.
250 2016b). The three different subregions are represented by $n_{\text{all}} = 14\text{-}18$ proxy records each, feature a
251 comparable density of proxy sites and the 6 closest neighbors to each site are at an average distance²
252 of less than 500 km. For the three clusters Northeastern (NE) Tibetan Plateau, Northcentral (NC) China
253 and Southeastern (SE) China we calculated arithmetic means with different subsets of proxy data. By
254 using a simple arithmetic mean for spatial aggregation, we have not taken advantage of more complex
255 aggregation strategies as employed in some reconstruction methods in order to keep the impact of
256 single records as transparent as possible. In order to estimate the overall suitability of proxy records,

² With exception from the borderline records #7, #25 and #55 (see Tab. 1).

257 we average records from the previously defined classes (good = +1; intermediate = 0; insufficient = -
258 1) of DA and EC. Besides the average of all records within each of the subregions (ave_{all}), we also
259 calculated an average with the most suitable records indicated by a classification index >0 (ave_{suit}). This
260 procedure reduced n_{all} to $n_{suit}=6-7$. To illustrate the range of variability when subsampling a small
261 population (i.e. all proxy records from one subregion) we calculated spatial averages from random
262 subsets of the proxy network. In a bootstrapped resampling with replacement, we made 1000 draws
263 of the size n_{suit} from n_{all} available records. We use the expressed population signal (EPS), a measure
264 adapted from dendrochronological applications (Wigley et al., 1984), to estimate how well the selected
265 records are able to represent the common signal of different subregions in the 1000-1900 CE period.
266 EPS is sensitive to the number of underlying records and to the mean correlation between these
267 records. For positive mean interseries correlations, it varies between 0 and 1, where 1 indicates a
268 perfect representation of the common signal.

269

270 **3. Results and discussion**

271 **3.1 Classification of proxy records**

272 Terrestrial proxies from Monsoon Asia differ significantly with respect to their DA (Table 1 and Fig. 2).
273 The highest DA was, unsurprisingly, found for documentary and tree-ring data. In documentary
274 records, dates are reported together with the observations, ruling out almost entirely the potential for
275 dating inaccuracy. However, some of the documentary records are of lower temporal resolution
276 because of the integration of observed extreme events over a certain time period (e.g. Zheng et al.
277 (2006) present a time-series with data every 20 years). In tree-ring chronologies a dating error due to
278 false counting or missing rings can be ruled out by cross-dating many trees from multiple sites
279 (Anchukaitis et al., 2012; Büntgen et al., 2018). The dating precision of other proxy archives differs
280 considerably. Some lake records derive their age-models from radiocarbon dating on bulk sediment
281 leading to age errors potentially in the range of multiple centuries (e.g. Liu et al., 2009) due to reservoir

282 effects in the water column. Laminations, in contrast, can decrease the age uncertainty of radiocarbon
283 or U/Th dates significantly. The U/Th-dated chronology of the speleothem record from Heshang cave
284 (Hu et al., 2008), for example, is validated by additional lamina counting. Such features can remain
285 unnoticed if only quantitative information about the age model (i.e. number and precision of dates)
286 are taken into account to assess the DA of a proxy record. Here, they are considered by lowering
287 (reservoir effects) or raising (lamination) the DA class by one step.

288 Regarding the EC, tree-ring records rank high again (Table 1). Annual resolution usually warrants
289 sufficient overlap with instrumental data and allows a straightforward verification of the climatic
290 signal. The same applies, but to a somewhat lesser extent, to other high-resolution natural proxy
291 records from speleothems or ice cores. For records with lower resolution, the climatic interpretation
292 is often based on a mechanistic understanding of the proxy. However, the effort made to verify the
293 climate signal varies significantly among different studies. All speleothem records in this study use $\delta^{18}\text{O}$
294 as a proxy for precipitation. This relationship is relatively well understood and in two studies supported
295 by evidence from monitoring experiments (Paulsen et al., 2003; Kuo et al., 2011), which results in an
296 intermediate EC ranking. Additionally, all speleothem studies illustrate the agreement with other,
297 nearby proxy records, which gives more confidence in their climate signal. Records from lake
298 sediments reveal a large variety of proxy types. Although some studies present a solid mechanistic
299 framework, regional comparisons are often more difficult because not only the proxy but also the
300 targeted hydrological parameter (e.g. precipitation, drought or runoff) can be different. This might
301 result in a different course of past hydroclimate and might impact the probability distribution and/or
302 frequency spectra of the data. All pollen records used in this study are derived from lake records. Most
303 of them are calibrated to annual precipitation amounts via today's pollen distributions. If only pollen
304 ratios are presented (e.g. Lake Aibi and Wulungu), there is a risk of underestimating the complexity of
305 pollen/climate interactions (Herzschuh, 2007). Hence, the EC for these pollen records was -1 or 0.

306

307 ***3.2 Comparison with 530 years of gridded precipitation***

308 To test whether the DA and EC classification is meaningful for the suitability of proxy records, we assess
309 the agreement with Shi17 in the low ($\geq \sim 100$ years) and mid (~ 10 -100 years) frequency domains.
310 Almost all documentary and tree-ring records from our setup correlate significantly with Shi17 in the
311 mid-frequency domain ($p=0.1$, one-sided Spearman), which is likely in some, but not all, cases a result
312 of data overlap (Fig. 2). However, half of the documentary data - those with $EC \leq 0$ - do not agree with
313 the target at centennial frequencies, supporting our suitability classification. This illustrates the
314 difficulty to reconstruct frequency domains beyond the length of the instrumental calibration period
315 (Fig. 2a-b). Among the records independent from Shi17, variability at time-scales greater than 100
316 years correlates significantly with Shi17 in 32% of the proxy records (Fig. 2a-b). Insufficiently dated
317 speleothem records show the lowest correlation values with Shi17 which is an indication that a good
318 dating is of importance also on longer time-scales.

319 Records from archives without a precise age-control are mostly limited in their ability to reflect decadal
320 scale variability in the precipitation data from Shi17 (Fig. 2c-d). Besides dating errors, this can be
321 related to the nonlinear influence of temperature changes (e.g. Paulsen et al., 2003). Likewise, the
322 precipitation reconstruction itself is likely not independent from temperature since the tree-rings used
323 for the reconstruction are drought sensitive in some regions. Further, the documentary data are not
324 precipitation measurements but presented as "drought and flood" events (Qian et al., 2003; Zheng et
325 al., 2006). Despite differences in the hydroclimatic target, six out of 18 lake sediment records show
326 significant correlations with Shi17 in the mid frequency domain, although their DA was ranked as
327 insufficient (Fig. 2c).

328 The overall weak correlation of lake sediment, speleothem, pollen and ice core records with
329 reconstructed precipitation (Fig. 2) is likely a result of uncertainties in the precipitation reconstruction
330 and in the proxy time-series. Slight differences regarding the targeted hydroclimatic parameter further
331 complicate the relationship. Reducing the length of the correlation period does not improve the
332 results, although the reconstruction is presumably more robust in the more recent centuries with a
333 more complete proxy network (results not shown).

334

335 **3.3 Correlation within the proxy network**

336 If DA and EC can inform about the suitability, those records with good DA and EC performance should
337 correlate more strongly with their neighbors than those records with a low suitability. Indeed, we find
338 higher correlations among more suitable records (Fig. 3). However, the discrimination between classes
339 is not distinct. A few records that scored high in the suitability classification (Fig. 2) reveal low
340 correlations with their neighbors and vice versa. A low correlation does not necessarily indicate that
341 the record has a weak climate signal or an incorrect dating. A mismatch can also be the result of poor
342 quality hydroclimate proxies among the neighboring records and/or spatially inhomogeneous
343 hydroclimate variability. Tree-ring and documentary data exhibit a decorrelation pattern in the 10-100
344 years frequency domain, indicating that the spatial relationship between records is limited to 500-700
345 km for decadal to multi-decadal variability (Fig. 3c,d), which is in agreement with previous results for
346 these latitudes (Ljungqvist et al., 2016; Talento et al., 2019). Orographic features and the spatial extent
347 of climate regimes can alter the length of correlation decay as shown with tree-rings (Cook et al., 2010).
348 Our results reveal that the decorrelation pattern also depends on the analyzed frequency domain (Fig.
349 3a,c). At centennial frequencies, the correlation decay becomes less distinct and significant
350 correlations are found even between records that are on average almost 1000 km away. Significantly
351 negative correlations in both frequency domains could reflect the high spatial variability of
352 hydroclimate within this region or records with insufficient DA and/or EC could spuriously correlate
353 with their neighbors (Fig. 3a,b).

354 For decadal to multidecadal variability, only tree-ring and documentary records yield significant
355 correlations with their neighbors (Fig. 3c,d). Records from these archives often correlate strongly in
356 the low frequency domain, too (Fig. 3a,b). Many lake sediment records agree well with their neighbors
357 on long timescales, despite low DA (Fig. 3a). Among speleothem data, high and low DA roughly
358 separates strongly and weakly correlating records (Fig. 3a), confirming the tendency found in the
359 correlations with Shi17 (Fig. 2). Records with low EC show no significant ($p \leq 0.01$) positive correlations

360 in the low and mid frequency domain (Fig. 3b,d). Correlation results in this experiment have to be
361 interpreted with caution: a low correlation with neighboring records can be caused by too much noise
362 in the neighbors' average and does not necessarily imply that the record of interest is unsuitable.

363 Evaluating proxy records based on "expert assessment" from the source publications yields, on
364 average, a reasonable suitability estimate. However, correlations with Shi17 and within the proxy
365 network reveal a considerable chance for incorrect classifications. Remarkably, many lake sediment
366 records from the lowest DA class showed strong coherency to Shi17 and/or within the proxy network
367 on centennial timescales implying that records with high dating uncertainty may still be dated properly.
368 Overestimating the suitability is likewise possible, if, for example, studies report a good EC, while the
369 records' climate signal becomes weaker back in time. This is typical of many tree-ring records because
370 the calibration period is normally based on a large number of trees (Esper et al., 2018) but the sample
371 size declines further back in time because of the limited availability of old living trees, historical timbers
372 or subfossil tree-trunks (Esper et al., 2016). For the cluster of speleothem records in southern China,
373 EC can be overestimated, too: in most studies, validation is achieved via high coherency with
374 neighboring speleothem records, but this coherency might arise from a coherent isotopic signal due
375 to common moisture sources in this region (Maher, 2008), rather than coherent rainfall amounts. Such
376 a conclusion is supported by the fact that the only southern China speleothem record with a high intra-
377 network correlation (#13) is the one in the center of multiple other speleothem isotope records. In
378 contrast, the lake sediment records with high intra-network correlations are spread over the entire
379 study region and cohere with records from different archives.

380 Classifying the suitability seems particularly valid for studying climate variability at multi-centennial to
381 millennial time-scales. At decadal to multidecadal scales performance is mainly determined by the
382 proxy type, i.e. only tree-ring chronologies and documentary data revealed robust evaluation results
383 (Fig. 2c,d; Fig. 3c,d). For longer-term variability, in contrast, the suitability classification seems to be
384 relevant for the choice of speleothem, documentary and tree-ring records. Both categories, DA and
385 EC, contribute important information and it is not possible to favor one criterion over the other based

386 on the results of this study. EC discriminated well, for example, between documentary records with
387 and without a significant correlation with Shi17 at low frequencies. DA performed better regarding the
388 classification of speleothem records. Thus, we combined the information from DA and EC in one
389 suitability measure for proxy selection.

390

391 **3.4 Autocorrelation in filtered and resampled time-series**

392 After smoothing and resampling the proxy data for the above analyses, the data are more
393 homogeneous regarding their frequency spectra. However, the proxy type still strongly affects the
394 autocorrelation of the low-pass filtered data (Fig. 4a), indicating that millennium-long trends might be
395 estimated differently depending on the dominating proxy-type. Averaged over all records from the
396 same archive, autocorrelation at lag 1 (i.e. 10 and 50 years for band- and low-pass filtered series)
397 ranges from 0.06 for tree-rings to 0.74 for lake sediments (Fig. 4a). Records from speleothems, pollen
398 and ice-core records reveal significant autocorrelations in the low frequency domain, too, whereas
399 documentary data can reach as low autocorrelations as tree-rings although the mean is slightly higher.
400 These findings may reflect an underestimation of long-term trends in documentary (Brázdil et al., 2005)
401 and tree-ring data (Cook et al., 1995; Klippel et al., 2019) as mentioned earlier. For the high
402 autocorrelation values in the other archives it cannot be ruled out that there is additional memory
403 induced by long-term processes in the hydrological, ecological or geological system that are not
404 primarily under climatic control. However, it is unlikely that high autocorrelation values in lake
405 sediment data are purely the result of non-climatic biases, because the low frequency signal in some
406 of these records revealed considerable coherency with Shi17 and with neighboring proxy records.
407 Potentially, higher autocorrelation is the result of a redder temperature frequency spectrum (Franke
408 et al. 2013, Zhang et al., 2015) that affects some, but not all records. Tree-rings from the Northeastern
409 Tibetan Plateau which are known to be partly temperature sensitive (Shao, 2005; Zhang et al., 2011;
410 Cook et al., 2013; Yang et al., 2014b; Duan et al., 2017; Duan et al. 2018) still reveal very low
411 autocorrelation values.

412 Diverging autocorrelation patterns are also visible in records classified based on the suitability criteria.
413 In particular, DA resembles the previously described pattern (Fig. 4a,b), because in DA mainly tree-ring
414 and documentary records return the highest suitability grade. For band-pass filtered data the overall
415 results are the same, although autocorrelation is generally lower in this domain for all cases (Fig. 4a-
416 c). The distinct offset in autocorrelation seems to be mostly a result of proxy characteristics. Therefore,
417 it is not possible to determine whether the lower autocorrelation in higher suitability classes or the
418 higher autocorrelation in lower suitability classes is closer to the truth. Only a combination of different
419 proxy types and archives might overcome such constraints.

420

421 ***3.5 Effects of proxy selection based on the suitability assessment***

422 By separating Monsoon Asia into subregions, we assess where and when constraining the number of
423 proxy records using DA and EC classes is useful. Based on the better evaluation results in the low
424 frequency domain (Fig. 2a,b; Fig. 3 a,b), we test the effects of using full versus reduced proxy networks
425 for only the low-pass filtered data. For each subregion, the full and reduced regional means are
426 discussed with respect to their archive composition, their long-term trends and their EPS-values.

427 The first subregion is located over the NE Tibetan Plateau (Fig. 1) and is represented by six lake
428 sediment, one pollen and seven tree-ring records (Fig. 5a). The average of all records from this region
429 indicates a long-term wetting trend from the onset to the end of the last millennium, as found by Chen
430 et al. (2015b) and Ljungqvist et al. (2016). If records of “insufficient” or “intermediate” suitability are
431 removed, the region is only represented by tree-ring data. The homogeneous hydroclimate signal
432 among tree-ring chronologies results in an increased EPS value despite using fewer records (Table 2
433 and Fig. 5a,b). The most pronounced difference between the reduced (only suitable records) and the
434 full (all records) average occurs around 1400 CE, when tree-rings indicate a pluvial period and most
435 other records imply dry to very dry conditions (Fig. 5a). Despite yielding a high EPS value, dismissing
436 non-tree-ring proxy records is problematic in this example for the following reasons. First, tree-rings
437 are not distributed over the entire subregion, so that the reduced average increases the risk of missing

438 climate variability of areas not covered by tree-rings. Second, the reduced average has a less distinct
439 millennial trend (Fig. 5b). This could be closer to the true climatic signal, but it could likewise result
440 from tree-ring data processing, that often confines the ability of tree-rings to represent trends on these
441 time-scales (Cook et al., 1995). Esper et al. (2016) showed that the characteristics of tree-ring samples
442 from the Tibetan Plateau would limit their ability to reproduce millennial length trends. An average of
443 the five lake sediment records from this region has a significant trend towards wetter conditions,
444 indicating that the tree-ring estimate is probably insufficient in this case (Fig. 5a). Thus, in this region
445 an average of all records seems the better choice despite the lower EPS value.

446 The second subregion covers NC China (Fig. 1) and is represented by four lake sediment, four
447 speleothem, seven documentary and three pollen records (Fig. 5c). The region overlaps with the
448 northern pole of the “North-South mode of hydroclimate variability” (Chen et al., 2015b) and
449 accordingly reveals a trend towards dryer conditions over the past millennium. Using only “suitable”
450 records yields an abrupt shift in the 15th century from a pluvial first half of the last millennium to a
451 drier second half (Fig. 5c,d). Considering all records, this transformation becomes more gradual with
452 wettest conditions around 1200 CE and driest around 1500 CE, while the amplitude remains the same.
453 At the same time, variability at centennial timescales is smaller for the full average. Together, these
454 findings indicate a limited ability of less suitable sediment archives or speleothems to resolve such
455 fluctuations, possibly due to longer-term environmental adjustments (Cai et al., 2010; Kasper et al.,
456 2012). Despite a lower EPS value (Table 2), the significantly enhanced centennial scale variability is an
457 argument for using the reduced average for this subregion, including 4 documentary, 1 pollen and 1
458 speleothem records.

459 The third subregion in the SE Chinese lowlands (Fig. 1) features seven documentary and five
460 speleothem records as well as two southern lake sediment records from coastal locations (Fig. 5e). The
461 southern counterpart of the “North-South mode of hydroclimate variability” is expected to show a
462 relatively dry onset of the last millennium and a wetting trend towards the Little Ice Age (Chen et al.,
463 2015b), which is confirmed by the full average of the proxy network in this region (Fig. 5f). The reduced

464 average, a mix of documentary and speleothem data, mimics the average of all data most closely
465 compared to the other two subregions (Fig. 5 b,d,f). The wettest and driest conditions occur in the
466 same epochs and both averages feature a similar millennial-long trend. In contrast to the NE Tibetan
467 Plateau, the records in the reduced average represent two different archives, which gives more
468 confidence in the results. However, the difference between the reduced and full average are rather
469 small throughout much of the last millennium so that both approaches seem valid for this example,
470 although the EPS value is significantly smaller for the reduced average.

471 The three subregions reveal that proxy filtering can only improve the common hydroclimate signal of
472 the network if high quality proxies are distributed over most of the spatial extent and if the region
473 features high quality proxies from various archives. Although these conditions were met in two out of
474 three subregions, the full average can still have a higher signal strength as indicated by the higher EPS
475 value. However, the EPS values in this study are generally weak and should not be over interpreted.
476 Compared to an application of EPS in a dendrochronological context, the sample size is rather small,
477 the number of time steps very limited and the signal to noise ratio low.

478 Proxy selection based on our suitability classes apparently requires a denser proxy network
479 encouraging further initiatives to sample and analyze more proxy archives. This is particularly
480 important for proxy systems sensitive for hydroclimatic changes. Our results reveal distinct divergence
481 between different archives in all subregions even though Monsoon Asia currently contains one of the
482 densest networks of millennial long hydroclimatic proxy records.

483

484 **4. Conclusions**

485 Proxy selection constitutes an important step in large-scale paleoclimatology. Relying solely on a
486 screening against instrumental data can penalize proxies that are of low temporal resolution. Including
487 all available data, in contrast, might introduce excessive amounts of noise from unsuitable proxy
488 records. We here suggest a method for proxy record evaluation that is based on meta information

489 derived from the associated publications. With the evaluation categories “dating accuracy” (DA) and
490 “evidence for a climate signal” (EC), two transparent and universal categories are developed that help
491 to identify records that contain a useful hydroclimatic signal over the last millennium. We test the DA
492 and EC classification using a partly independent hydroclimatic reconstruction as well as intra-network
493 correlations. Suitability estimates for tree-ring, speleothem and documentary records contain valuable
494 information. The classification of lake sediments is more prone to an underestimation of their actual
495 suitability. Some significant correlations with records from other archives are achieved despite large
496 dating uncertainties. Documentary and tree-ring data reveal the best classification results for DA and
497 EC. However, their weak autocorrelation on centennial timescales is likely associated with inherent
498 limitations of these proxy types. The existence of long-term memory in hydroclimate is suggested by
499 the robust intra-network correlations found in some lake sediment records.

500 In order to reproduce climate variability at all timescales we encourage the application of multi proxy
501 compilations in our Monsoon Asia study region. Besides improved frequency spectra, the integration
502 of various proxy archives will also increase the spatial coverage. A dense proxy network is of particular
503 importance for hydroclimate reconstructions due to the short correlation decay length, which we
504 proofed with intra-network correlations of documentary and tree-ring data. Our analyses of different,
505 well-sampled subregions corroborates that only a well balanced mix of different proxies yields
506 favorable characteristics of spatial averages. Selecting a subset of records based on the previously
507 defined suitability classes does not improve the signal strength, but it might reveal noteworthy
508 differences between the full and the reduced average.

509 Although the millennium long hydroclimatic proxy network in Monsoon Asia is not yet dense enough
510 for a proxy selection based on our suitability criteria, this approach can be transferred to other large-
511 scale paleoclimate studies. The global proxy network is constantly growing. DA and EC offer guidance
512 in the process of proxy selection. They can be assessed for many different types of paleoclimate
513 records and their specification can be adjusted to different problems.

514

515 **Acknowledgements**

516 L.S., S.T., T.J.O., B.Y. and J.L. are supported by the Belmont Forum and JPI-Climate, Collaborative
517 Research Action “INTEGRATE An integrated data–model study of interactions between tropical
518 monsoons and extratropical climate variability and extremes” (BMBF grant no. 01LP1612A; NERC
519 grant no. NE/P006809/1; NSFC grant no. 41661144008). F.C.L. was supported by the Swedish
520 Research Council (Vetenskapsrådet, grant no. 2018-01272). J.L. acknowledges also the Climate
521 Science for Service Partnership China project (CSSP China). We declare that the authors have no
522 competing interests. Author contributions: L.S. and J.L. conceptualized the study; F.C.L., B.Y., F.C.,
523 J.C., J.L., Z.H. and Q.G. contributed and curated data; L.S. analyzed and investigated the data; L.S.
524 wrote the original draft; all authors contributed to the discussion and interpretation of the results
525 and to the editing process.

- 527 Academy of Meteorological Science, 1981. Yearly Charts of Dryness/Wetness in China for the Last 500-
528 Year Period. China Cartographic Publishing House Beijing, China.
- 529 Anchukaitis, K.J., Breitenmoser, P., Briffa, K.R., Buchwal, A., Büntgen, U., Cook, E.R., D'Arrigo, R.D.,
530 Esper, J., Evans, M.N., Frank, D., Grudd, H., Gunnarson, B.E., Hughes, M.K., Kirilyanov, A.V.,
531 Körner, C., Krusic, P.J., Luckman, B., Melvin, T.M., Salzer, M.W., Shashkin, A.V., Timmreck, C.,
532 Vaganov, E.A., Wilson, R.J.S., 2012. Tree rings and volcanic cooling. *Nat. Geosci.* 5, 836–837.
533 <https://doi.org/10.1038/ngeo1645>
- 534 Brázdil, R., Kiss, A., Luterbacher, J., Nash, D. J., Řezníčková, L., 2018. Documentary data and the study
535 of the past droughts: an overview of the state of the art worldwide. *Clim. Past* 14, 1915–1960.
536 <https://doi.org/10.5194/cp-14-1915-2018>
- 537 Brázdil, R., Pfister, C., Wanner, H., Storch, H.V., Luterbacher, J., 2005. Historical Climatology In Europe
538 – The State Of The Art. *Clim. Change* 70, 363–430. <https://doi.org/10.1007/s10584-005-5924-1>
- 539 Bunde, A., Büntgen, U., Ludescher, J., Luterbacher, J., von Storch, H., 2013. Is there memory in
540 precipitation? *Nat. Clim. Change* 3, 174–175. <https://doi.org/10.1038/nclimate1830>
- 541 Bunn, A.G., 2010. Statistical and visual crossdating in R using the dplR library. *Dendrochronologia* 28,
542 251–258. <https://doi.org/10.1016/j.dendro.2009.12.001>
- 543 Büntgen, U., Franke, J., Frank, D., Wilson, R., González-Rouco, F., Esper, J., 2010. Assessing the spatial
544 signature of European climate reconstructions. *Clim. Res.* 41, 125–130.
545 <https://doi.org/10.3354/cr00848>
- 546 Büntgen, U., Wacker, L., Galván, J.D., Arnold, S., Arseneault, D., Baillie, M., Beer, J., Bernabei, M.,
547 Bleicher, N., Boswijk, G., Bräuning, A., Carrer, M., Ljungqvist, F.C., Cherubini, P., Christl, M.,
548 Christie, D.A., Clark, P.W., Cook, E.R., D'Arrigo, R., Davi, N., Eggertsson, Ó., Esper, J., Fowler,
549 A.M., Gedalof, Z., Gennaretti, F., Gieblinger, J., Grissino-Mayer, H., Grudd, H., Gunnarson, B.E.,
550 Hantemirov, R., Herzig, F., Hessler, A., Heussner, K.-U., Jull, A.J.T., Kukarskih, V., Kirilyanov, A.,
551 Kolář, T., Krusic, P.J., Kyncl, T., Lara, A., LeQuesne, C., Linderholm, H.W., Loader, N.J., Luckman,

552 B., Miyake, F., Myglan, V.S., Nicolussi, K., Oppenheimer, C., Palmer, J., Panyushkina, I.,
553 Pederson, N., Rybníček, M., Schweingruber, F.H., Seim, A., Sigl, M., Churakova, O., Speer, J.H.,
554 Synal, H.-A., Tegel, W., Treydte, K., Villalba, R., Wiles, G., Wilson, R., Winship, L.J., Wunder, J.,
555 Yang, B., Young, G.H.F., 2018. Tree rings reveal globally coherent signature of cosmogenic
556 radiocarbon events in 774 and 993 CE. *Nat. Commun.* 9. [https://doi.org/10.1038/s41467-018-](https://doi.org/10.1038/s41467-018-06036-0)
557 06036-0

558 Cai, Y., Tan, L., Cheng, H., An, Z., Edwards, R.L., Kelly, M.J., Kong, X., Wang, X., 2010. The variation of
559 summer monsoon precipitation in central China since the last deglaciation. *Earth Planet. Sci.*
560 *Lett.* 291, 21–31. <https://doi.org/10.1016/j.epsl.2009.12.039>

561 Chen, F., Huang, X., Zhang, J., Holmes, J.A., Chen, J., 2006. Humid Little Ice Age in arid central Asia
562 documented by Bosten Lake, Xinjiang, China. *Sci. China Ser. Earth Sci.* 49, 1280–1290.
563 <https://doi.org/10.1007/s11430-006-2027-4>

564 Chen, F., Xu, Q., Chen, J., Birks, H.J.B., Liu, J., Zhang, S., Jin, L., An, C., Telford, R.J., Cao, X., Wang, Z.,
565 Zhang, X., Selvaraj, K., Lu, H., Li, Y., Zheng, Z., Wang, H., Zhou, A., Dong, G., Zhang, J., Huang,
566 X., Bloemendal, J., Rao, Z., 2015a. East Asian summer monsoon precipitation variability since
567 the last deglaciation. *Sci. Rep.* 5. <https://doi.org/10.1038/srep11186>

568 Chen, J., Chen, F., Feng, S., Huang, W., Liu, J., Zhou, A., 2015b. Hydroclimatic changes in China and
569 surroundings during the Medieval Climate Anomaly and Little Ice Age: spatial patterns and
570 possible mechanisms. *Quat. Sci. Rev.* 107, 98–111.
571 <https://doi.org/10.1016/j.quascirev.2014.10.012>

572 Chen, J., Chen, F., Zhang, E., Brooks, S.J., Zhou, A., Zhang, J., 2009. A 1000-year chironomid-based
573 salinity reconstruction from varved sediments of Sagan Lake, Qaidam Basin, arid Northwest
574 China, and its palaeoclimatic significance. *Chin. Sci. Bull.* 54, 3749–3759.
575 <https://doi.org/10.1007/s11434-009-0201-8>

576 Cheng, H., Zhang, P.Z., Spötl, C., Edwards, R.L., Cai, Y.J., Zhang, D.Z., Sang, W.C., Tan, M., An, Z.S., 2012.
577 The climatic cyclicity in semiarid-arid central Asia over the past 500,000 years. *Geophys. Res.*
578 *Lett.* 39, n/a-n/a. <https://doi.org/10.1029/2011GL050202>

579 Christiansen, B., Ljungqvist, F.C., 2012. The extra-tropical Northern Hemisphere temperature in the
580 last two millennia: reconstructions of low-frequency variability. *Clim. Past* 8, 765–786.

581 Christiansen, B., Ljungqvist, F.C., 2017. Challenges and perspectives for large-scale temperature
582 reconstructions of the past two millennia. *Rev. Geophys.* 55, 40–96.
583 <https://doi.org/10.1002/2016RG000521>

584 Chu, G., Sun, Q., Wang, X., Li, D., Rioual, P., Qiang, L., Han, J., Liu, J., 2009. A 1600 year multiproxy
585 record of paleoclimatic change from varved sediments in Lake Xiaolongwan, northeastern
586 China. *J. Geophys. Res.* 114. <https://doi.org/10.1029/2009JD012077>

587 Compo, G.P., Whitaker, J.S., Sardeshmukh, P.D., Matsui, N., Allan, R.J., Yin, X., Gleason, B.E., Vose, R.S.,
588 Rutledge, G., Bessemoulin, P., Brönnimann, S., Brunet, M., Crouthamel, R.I., Grant, A.N.,
589 Groisman, P.Y., Jones, P.D., Kruk, M.C., Kruger, A.C., Marshall, G.J., Maugeri, M., Mok, H.Y.,
590 Nordli, Ø., Ross, T.F., Trigo, R.M., Wang, X.L., Woodruff, S.D., Worley, S.J., 2011. The Twentieth
591 Century Reanalysis Project. *Q. J. R. Meteorol. Soc.* 137, 1–28. <https://doi.org/10.1002/qj.776>

592 Conroy, J.L., Hudson, A.M., Overpeck, J.T., Liu, K.-B., Wang, L., Cole, J.E., 2017. The primacy of
593 multidecadal to centennial variability over late-Holocene forced change of the Asian Monsoon
594 on the southern Tibetan Plateau. *Earth Planet. Sci. Lett.* 458, 337–348.
595 <https://doi.org/10.1016/j.epsl.2016.10.044>

596 Cook, E.R., Anchukaitis, K.J., Buckley, B.M., D’Arrigo, R.D., Jacoby, G.C., Wright, W.E., 2010. Asian
597 Monsoon Failure and Megadrought During the Last Millennium. *Science* 328, 486–489.
598 <https://doi.org/10.1126/science.1185188>

599 Cook, E.R., Briffa, K.R., Meko, D.M., Graybill, D.A., Funkhouser, G., 1995. The “segment length curse”
600 in long tree-ring chronology development for palaeoclimatic studies. *Holocene* 5, 229–237.
601 <https://doi.org/10.1177/095968369500500211>

602 Cook, E.R., D’Arrigo, R.D., Mann, M.E., 2002. A Well-Verified, Multiproxy Reconstruction of the Winter
603 North Atlantic Oscillation Index since A.D. 1400. *J. Climate* 15, 1754–1764.
604 [https://doi.org/10.1175/1520-0442\(2002\)015<1754:AWVMRO>2.0.CO;2](https://doi.org/10.1175/1520-0442(2002)015<1754:AWVMRO>2.0.CO;2)

605 Cook, E.R., Krusic, P.J., Anchukaitis, K.J., Buckley, B.M., Nakatsuka, T., Sano, M., PAGES Asia2k
606 Members, 2013. Tree-ring reconstructed summer temperature anomalies for temperate East
607 Asia since 800 C.E. *Clim. Dyn.* 41, 2957–2972. <https://doi.org/10.1007/s00382-012-1611-x>

608 Cook, E.R., Peters, K., 1981. The smoothing spline: a new approach to standardizing forest interior tree-
609 ring width series for dendroclimatic studies. *Tree-Ring Bull.* 41, 45–53.

610 Datta, S., Jones, W. L., Roy, B., Tokay, A., 2003. Spatial variability of surface rainfall as observed from
611 TRMM field campaign data. *J. Appl. Meteorol.* 42, 598–610. [https://doi.org/10.1175/1520-0450\(2003\)042<0598:SVOSRA>2.0.CO;2](https://doi.org/10.1175/1520-0450(2003)042<0598:SVOSRA>2.0.CO;2)

613 Dienst, M., Lindén, J., Engström, E., Esper, J., 2017. Removing the relocation bias from the 155-year
614 Haparanda temperature record in Northern Europe. *Int. J. Climatol.* 37, 4015–4026.
615 <https://doi.org/10.1002/joc.4981>

616 Dobrovolný, P., Moberg, A., Brázdil, R., Pfister, C., Glaser, R., Wilson, R., van Engelen, A., Limanówka,
617 D., Kiss, A., Halíčková, M., Macková, J., Riemann, D., Luterbacher, J., Böhm, R., 2010. Monthly,
618 seasonal and annual temperature reconstructions for Central Europe derived from
619 documentary evidence and instrumental records since AD 1500. *Clim. Change* 101, 69–107.
620 <https://doi.org/10.1007/s10584-009-9724-x>

621 Duan, J., Esper, J., Büntgen, U., Li, L., Xoplaki, E., Zhang, H., Wang, L., Fang, Y., Luterbacher, J., 2017.
622 Weakening of annual temperature cycle over the Tibetan Plateau since the 1870s. *Nature*
623 *Comm.*, 8: 14008. <https://doi.org/10.1038/ncomms14008>

624 Duan, J., Li, L., Ma, Z., Esper, J., Büntgen, U., Xoplaki, E., Zhang, D., Wang, L., Yin, H., Luterbacher, J.,
625 2018. Summer Cooling Driven by Large Volcanic Eruptions over the Tibetan Plateau. *J. Clim.*
626 31, 9869–9879. <https://doi.org/10.1175/JCLI-D-17-0664.1>

627 Esper, J., Cook, E.R., Krusic, P.J., Peters, K., Schweingruber, F.H., 2003. Tests of the RCS method for
628 preserving low-frequency variability in long tree-ring chronologies. *Tree-Ring Res.* 59: 81-98.

629 Esper, J., Frank, D., 2009. Divergence pitfalls in tree-ring research. *Clim. Change* 94, 261–266.
630 <https://doi.org/10.1007/s10584-009-9594-2>

631 Esper, J., Frank, D., Büntgen, U., Verstege, A., Luterbacher, J., Xoplaki, E., 2007. Long-term drought
632 severity variations in Morocco. *Geophys. Res. Lett.* 34.
633 <https://doi.org/10.1029/2007GL030844>

634 Esper, J., George, S.S., Anchukaitis, K., D'Arrigo, R., Ljungqvist, F.C., Luterbacher, J., Schneider, L.,
635 Stoffel, M., Wilson, R., Büntgen, U., 2018. Large-scale, millennial-length temperature
636 reconstructions from tree-rings. *Dendrochronologia* 50, 81–90.
637 <https://doi.org/10.1016/j.dendro.2018.06.001>

638 Esper, J., Krusic, P.J., Ljungqvist, F.C., Luterbacher, J., Carrer, M., Cook, E., Davi, N.K., Hartl-Meier, C.,
639 Kirilyanov, A., Konter, O., Myglan, V., Timonen, M., Treydte, K., Trouet, V., Villalba, R., Yang,
640 B., Büntgen, U., 2016. Ranking of tree-ring based temperature reconstructions of the past
641 millennium. *Quat. Sci. Rev.* 145, 134–151. <https://doi.org/10.1016/j.quascirev.2016.05.009>

642 Feng, S., Hu, Q., Wu, Q., Mann, M.E., 2013. A Gridded Reconstruction of Warm Season Precipitation
643 for Asia Spanning the Past Half Millennium. *J. Clim.* 26, 2192–2204.
644 <https://doi.org/10.1175/JCLI-D-12-00099.1>

645 Feng, Z.-D., Wu, H.N., Zhang, C.J., Ran, M., Sun, A.Z., 2013. Bioclimatic change of the past 2500 years
646 within the Balkhash Basin, eastern Kazakhstan, Central Asia. *Quat. Int.* 311, 63–70.
647 <https://doi.org/10.1016/j.quaint.2013.06.032>

648 Frank, D., Büntgen, U., Böhm, R., Maugeri, M., Esper, J., 2007. Warmer early instrumental
649 measurements versus colder reconstructed temperatures: shooting at a moving target. *Quat.*
650 *Sci. Rev.* 26, 3298–3310. <https://doi.org/10.1016/j.quascirev.2007.08.002>

651 Frank, D., Esper, J., Zorita, E., Wilson, R., 2010. A noodle, hockey stick, and spaghetti plate: a
652 perspective on high-resolution paleoclimatology: A noodle, hockey stick, and spaghetti plate.
653 *Wiley Interdiscip. Rev. Clim. Change* 1, 507–516. <https://doi.org/10.1002/wcc.53>

654 Franke, J., Frank, D., Raible, C.C., Esper, J., Brönnimann, S., 2013. Spectral biases in tree-ring climate
655 proxies. *Nat. Clim. Change* 3, 360–364. <https://doi.org/10.1038/nclimate1816>

656 Ge, Q., Zheng, J., Tian, Y., Wu, W., Fang, X., Wang, W.-C., 2008. Coherence of climatic reconstruction
657 from historical documents in China by different studies. *Int. J. Climatol.* 28, 1007–1024.
658 <https://doi.org/10.1002/joc.1552>

659 Glaser, R., Riemann, D., 2009. A thousand-year record of temperature variations for Germany and
660 Central Europe based on documentary data. *J. Quat. Sci.* 24, 437–449.
661 <https://doi.org/10.1002/jqs.1302>

662 Gong, G., Hameed, S., 1991. The variation of moisture conditions in China during the last 2000 years.
663 *Int. J. Climatol.* 11, 271–283.

664 Gou, X., Deng, Y., Chen, F., Yang, M., Fang, K., Gao, L., Yang, T., Zhang, F., 2010. Tree ring based
665 streamflow reconstruction for the Upper Yellow River over the past 1234 years. *Chin. Sci. Bull.*
666 55, 4179–4186. <https://doi.org/10.1007/s11434-010-4215-z>

667 Hao, Z., Geng, X., Liu, K., Liu, H., Zheng, J., 2017. Dryness and wetness variations for the past 1000 years
668 in Guanzhong Plain. *Chin. Sci. Bull.* 62, 2399–2406. <https://doi.org/10.1360/N972017-00209>

669 Harris, I., Jones, P.D., Osborn, T.J., Lister, D.H., 2014. Updated high-resolution grids of monthly climatic
670 observations - the CRU TS3.10 Dataset. *Int. J. Climatol.* 34, 623–642.
671 <https://doi.org/10.1002/joc.3711>

672 He, Y., Zhao, C., Wang, Z., Wang, H., Song, M., Liu, W., Liu, Z., 2013. Late Holocene coupled moisture
673 and temperature changes on the northern Tibetan Plateau. *Quat. Sci. Rev.* 80, 47–57.
674 <https://doi.org/10.1016/j.quascirev.2013.08.017>

675 Herzschuh, U., 2007. Reliability of pollen ratios for environmental reconstructions on the Tibetan
676 Plateau. *J. Biogeogr.* 34, 1265–1273. <https://doi.org/10.1111/j.1365-2699.2006.01680.x>

677 Hu, C., Henderson, G.M., Huang, J., Xie, S., Sun, Y., Johnson, K.R., 2008. Quantification of Holocene
678 Asian monsoon rainfall from spatially separated cave records. *Earth Planet. Sci. Lett.* 266, 221–
679 232. <https://doi.org/10.1016/j.epsl.2007.10.015>

680 Jiang, T., Zhang, Q., Blender, R., Fraedrich, K., 2005. Yangtze Delta floods and droughts of the last
681 millennium: Abrupt changes and long term memory. *Theor. Appl. Climatol.* 82, 131–141.
682 <https://doi.org/10.1007/s00704-005-0125-4>

683 Kaspari, S., Mayewski, P., Kang, S., Sneed, S., Hou, S., Hooke, R., Kreutz, K., Introne, D., Handley, M.,
684 Maasch, K., Qin, D., Ren, J., 2007. Reduction in northward incursions of the South Asian
685 monsoon since ~1400 AD inferred from a Mt. Everest ice core. *Geophys. Res. Lett.* 34.
686 <https://doi.org/10.1029/2007GL030440>

687 Kasper, T., Haberzettl, T., Doberschütz, S., Daut, G., Wang, J., Zhu, L., Nowaczyk, N., Mäusbacher, R.,
688 2012. Indian Ocean Summer Monsoon (IOSM)-dynamics within the past 4 ka recorded in the
689 sediments of Lake Nam Co, central Tibetan Plateau (China). *Quat. Sci. Rev.* 39, 73–85.
690 <https://doi.org/10.1016/j.quascirev.2012.02.011>

691 Klippel, L., St. George, S., Büntgen, U., Krusic, P.J., Esper, J., 2019. Differing pre-industrial cooling trends
692 between tree-rings and lower-resolution temperature proxies. *Clim. Past Discuss.* 1–21.
693 <https://doi.org/10.5194/cp-2019-41>

694 Krusic, P.J., Cook, E.R., Dukpa, D., Putnam, A.E., Rupper, S., Schaefer, J., 2015. Six hundred thirty-eight
695 years of summer temperature variability over the Bhutanese Himalaya: Bhutan summer
696 temperature reconstruction. *Geophys. Res. Lett.* 42, 2988–2994.
697 <https://doi.org/10.1002/2015GL063566>

698 Kuo, T.-S., Liu, Z.-Q., Li, H.-C., Wan, N.-J., Shen, C.-C., Ku, T.-L., 2011. Climate and environmental
699 changes during the past millennium in central western Guizhou, China as recorded by
700 Stalagmite ZJD-21. *J. Asian Earth Sci.* 40, 1111–1120.
701 <https://doi.org/10.1016/j.jseaes.2011.01.001>

702 Li, H.-C., Lee, Z.-H., Wan, N.-J., Shen, C.-C., Li, T.-Y., Yuan, D.-X., Chen, Y.-H., 2011. The $\delta^{18}\text{O}$ and $\delta^{13}\text{C}$
703 records in an aragonite stalagmite from Furong Cave, Chongqing, China: A-2000-year record
704 of monsoonal climate. *J. Asian Earth Sci.* 40, 1121–1130.
705 <https://doi.org/10.1016/j.jseaes.2010.06.011>

706 Li, J., Dodson, J., Yan, H., Cheng, B., Zhang, X., Xu, Q., Ni, J., Lu, F., 2017a. Quantitative precipitation
707 estimates for the northeastern Qinghai-Tibetan Plateau over the last 18,000 years. *J. Geophys.*
708 *Res. Atmospheres* 122, 5132–5143. <https://doi.org/10.1002/2016JD026333>

709 Li, J., Dodson, J., Yan, H., Zhang, D.D., Zhang, X., Xu, Q., Lee, H.F., Pei, Q., Cheng, B., Li, C., Ni, J., Sun, A.,
710 Lu, F., Zong, Y., 2017b. Quantifying climatic variability in monsoonal northern China over the
711 last 2200 years and its role in driving Chinese dynastic changes. *Quat. Sci. Rev.* 159, 35–46.
712 <https://doi.org/10.1016/j.quascirev.2017.01.009>

713 Li, S., Wang, X., Xia, W., Li, W., 2004. The little ice age climate fluctuations derived from lake sediments
714 of Goulucuo, Qinghai-Xizang Plateau. *Quat. Sci.* 24, 578–584.

715 Liu, J., Chen, F., Chen, J., Xia, D., Xu, Q., Wang, Z., Li, Y., 2011. Humid medieval warm period recorded
716 by magnetic characteristics of sediments from Gonghai Lake, Shanxi, North China. *Chin. Sci.*
717 *Bull.* 56, 2464–2474. <https://doi.org/10.1007/s11434-011-4592-y>

718 Liu, X., Dong, H., Yang, X., Herzschuh, U., Zhang, E., Stuetz, J.-B.W., Wang, Y., 2009. Late Holocene forcing
719 of the Asian winter and summer monsoon as evidenced by proxy records from the northern
720 Qinghai-Tibetan Plateau. *Earth Planet. Sci. Lett.* 280, 276–284.
721 <https://doi.org/10.1016/j.epsl.2009.01.041>

722 Liu, X., Herzschuh, U., Shen, J., Jiang, Q., Xiao, X., 2008. Holocene environmental and climatic changes
723 inferred from Wulungu Lake in northern Xinjiang, China. *Quat. Res.* 70, 412–425.
724 <https://doi.org/10.1016/j.yqres.2008.06.005>

725 Ljungqvist, F.C., 2017. Human and Societal Dimensions of Past Climate Change, in: Crumley, C.L.,
726 Lennartsson, T., Westin, A. (Eds.), *Issues and Concepts in Historical Ecology: The Past and*
727 *Future of Landscapes and Regions.* Cambridge University Press, pp. 41–83.
728 <https://doi.org/10.1017/9781108355780.003>

729 Ljungqvist, F.C., Krusic, P.J., Brattström, G., Sundqvist, H.S., 2012. Northern Hemisphere temperature
730 patterns in the last 12 centuries. *Clim. Past* 8, 227–249. [https://doi.org/10.5194/cp-8-227-](https://doi.org/10.5194/cp-8-227-2012)
731 [2012](https://doi.org/10.5194/cp-8-227-2012)

732 Ljungqvist, F.C., Krusic, P.J., Sundqvist, H.S., Zorita, E., Brattström, G., Frank, D., 2016. Northern
733 Hemisphere hydroclimate variability over the past twelve centuries. *Nature* 532, 94–98.
734 <https://doi.org/10.1038/nature17418>

735 Luterbacher, J., Dietrich, D., Xoplaki, E., Grosjean, M., Wanner, H., 2004. European seasonal and annual
736 temperature variability, trends, and extremes since 1500. *Science*, 303: 1499-1503.
737 <https://doi.org/10.1126/science.1093877>

738 Luterbacher, J., Werner, J.P., Smerdon, J.E., Fernández-Donado, L., González-Rouco, F.J., Barriopedro,
739 D., Ljungqvist, F.C., Büntgen, U., Zorita, E., Wagner, S., Esper, J., McCarroll, D., Toreti, A., Frank,
740 D., Jungclaus, J.H., Barriendos, M., Bertolin, C., Bothe, O., Brázdil, R., Camuffo, D., Dobrovolný,
741 P., Gagen, M., García-Bustamante, E., Ge, Q., Gómez-Navarro, J.J., Guiot, J., Hao, Z., Hegerl,
742 G.C., Holmgren, K., Klimenko, V.V., Martín-Chivelet, J., Pfister, C., Roberts, N., Schindler, A.,
743 Schurer, A., Solomina, O., von Gunten, L., Wahl, E., Wanner, H., Wetter, O., Xoplaki, E., Yuan,
744 N., Zanchettin, D., Zhang, H., Zerefos, C., 2016. European summer temperatures since Roman
745 times. *Environ. Res. Lett.* 11, 024001. <https://doi.org/10.1088/1748-9326/11/2/024001>

746 Ma, J., Edmunds, W.M., 2006. Groundwater and lake evolution in the Badain Jaran Desert ecosystem,
747 Inner Mongolia. *Hydrogeol. J.* 14, 1231–1243. <https://doi.org/10.1007/s10040-006-0045-0>

748 Maher, B.A., 2008. Holocene variability of the East Asian summer monsoon from Chinese cave records:
749 a re-assessment. *Holocene* 18, 861–866. <https://doi.org/10.1177/0959683608095569>

750 Man, Z., 2009. Research on climate change during historical times in China. Shandong Education Press.

751 Masson-Delmotte, V., Schulz, M., Abe-Ouchi, A., Beer, J., Ganopolski, A., González Rouco, J.F., Jansen,
752 E., Lambeck, K., Luterbacher, J., Naish, T.R., Osborn, T., Otto-Bliesner, B.L., Quinn, T.M.,
753 Ramesh, R., Rojas, M., Shao, X., Timmermann, A., 2013. Information from Paleoclimate
754 Archives, in Stocker, T.F., Qin, D., Plattner, G.-K., Tignor, M., Allen, S.K., Doschung, J., Nauels,
755 A., Xia, Y., Bex, V., and Midgley, P.M. (Eds.), *Climate Change 2013: The Physical Science Basis.*
756 *Contribution of Working Group I to the Fifth Assessment Report of the Intergovernmental*
757 *Panel on Climate Change.* Cambridge University Press, Cambridge, pp. 383-464.
758 [doi:10.1017/CBO9781107415324.013](https://doi.org/10.1017/CBO9781107415324.013)

759 McDonald, J.E., Green, C.R., 1960. A comparison of rank-difference and product-moment correlation
760 of precipitation data. *J. Geophys. Res.* 65, 333–336. <https://doi.org/10.1029/JZ065i001p00333>

761 Melvin, T.M., Briffa, K.R., 2008. A “signal-free” approach to dendroclimatic standardisation.
762 *Dendrochronologia* 26, 71–86. <https://doi.org/10.1016/j.dendro.2007.12.001>

763 Moberg, A., Andersson, H., Bergström, H., Jones, P.D., 2003. Were southern Swedish summer
764 temperatures before 1860 as warm as measured? *Int. J. Climatol.* 23, 1495–1521.
765 <https://doi.org/10.1002/joc.945>

766 Neukom, R., Gergis, J., Karoly, D.J., Wanner, H., Curran, M., Elbert, J., González-Rouco, F., Linsley, B.K.,
767 Moy, A.D., Mundo, I., Raible, C.C., Steig, E.J., van Ommen, T., Vance, T., Villalba, R., Zinke, J.,
768 Frank, D., 2014. Inter-hemispheric temperature variability over the past millennium. *Nat. Clim.*
769 *Change* 4, 362–367. <https://doi.org/10.1038/nclimate2174>

770 PAGES2k Consortium, 2013. Continental-scale temperature variability during the past two millennia.
771 *Nat. Geosci.* 6, 339–346. <https://doi.org/10.1038/ngeo1797>

772 PAGES2k Consortium, 2017. A global multiproxy database for temperature reconstructions of the
773 Common Era. *Sci. Data* 4, 170088. <https://doi.org/10.1038/sdata.2017.88>

774 PAGES Hydro2k Consortium, 2017. Comparing proxy and model estimates of hydroclimate variability
775 and change over the Common Era. *Clim. Past* 13, 1851–1900. [https://doi.org/10.5194/cp-13-](https://doi.org/10.5194/cp-13-1851-2017)
776 [1851-2017](https://doi.org/10.5194/cp-13-1851-2017)

777 Parker, D.E., 1994. Effects of changing exposure of thermometers at land stations. *Int. J. Climatol.* 14,
778 1–31. <https://doi.org/10.1002/joc.3370140102>

779 Pauling, A., Luterbacher, J., Wanner, H., 2003. Evaluation of Proxies for European and North Atlantic
780 Temperature Field Reconstructions. *Geophys. Res. Lett.* 30, 1787–1790.
781 <https://doi.org/10.1029/2003GL017589>

782 Paulsen, D.E., Li, H.-C., Ku, T.-L., 2003. Climate variability in central China over the last 1270 years
783 revealed by high-resolution stalagmite records. *Quat. Sci. Rev.* 22, 691–701.
784 [https://doi.org/10.1016/S0277-3791\(02\)00240-8](https://doi.org/10.1016/S0277-3791(02)00240-8)

785 Pederson, N., Hessel, A.E., Baatarbileg, N., Anchukaitis, K.J., Di Cosmo, N., 2014. Pluvials, droughts, the
786 Mongol Empire, and modern Mongolia. *Proc. Natl. Acad. Sci.* 111, 4375–4379.
787 <https://doi.org/10.1073/pnas.1318677111>

788 Pfister, C., Camenisch, C., Dobrovolný, P., 2018. Analysis and Interpretation: Temperature and
789 Precipitation Indices, in: White, S., Pfister, C., Mauelshagen, F. (Eds.), *The Palgrave Handbook*
790 of Climate History. Palgrave Macmillan UK, London, pp. 115–129.
791 https://doi.org/10.1057/978-1-137-43020-5_11

792 Qian, W., Hu, Q., Zhu, Y., Lee, D.-K., 2003. Centennial-scale dry-wet variations in East Asia. *Clim. Dyn.*
793 21, 77–89. <https://doi.org/10.1007/s00382-003-0319-3>

794 Qin, J., Yuan, D., Lin, Y., Zhang, H., Zhang, M., Cheng, H., Wang, H., Yang, Y., Ran, J., 2008. High
795 resolution stalagmite records of climate change since 800 AD in Libo, Guizhou. *Carsologica Sin.*
796 27, 266–272.

797 Sanwal, J., Kotlia, B.S., Rajendran, C., Ahmad, S.M., Rajendran, K., Sandiford, M., 2013. Climatic
798 variability in Central Indian Himalaya during the last ~1800 years: Evidence from a high
799 resolution speleothem record. *Quat. Int.* 304, 183–192.
800 <https://doi.org/10.1016/j.quaint.2013.03.029>

801 Schneider, L., Smerdon, J.E., Büntgen, U., Wilson, R.J.S., Myglan, V.S., Kirdyanov, A.V., Esper, J., 2015.
802 Revising midlatitude summer temperatures back to A.D. 600 based on a wood density
803 network. *Geophys. Res. Lett.* 42, 4556–4562. <https://doi.org/10.1002/2015GL063956>

804 Shao, X., 2005. Reconstruction of precipitation variation from tree rings in recent 1000 years in
805 Delingha, Qinghai. *Sci. China Ser. D* 48, 939. <https://doi.org/10.1360/03yd0146>

806 Sheppard, P.R., Tarasov, P.E., Graumlich, L.J., Heussner, K.-U., Wagner, M., Österle, H., Thompson, L.G.,
807 2004. Annual precipitation since 515 BC reconstructed from living and fossil juniper growth of
808 northeastern Qinghai Province, China. *Clim. Dyn.* 23, 869–881.
809 <https://doi.org/10.1007/s00382-004-0473-2>

810 Shi, F., Zhao, S., Guo, Z., Goosse, H., Yin, Q., 2017. Multi-proxy reconstructions of precipitation field in
811 China over the past 500 years. *Clim. Past* 13, 1919–1938. [https://doi.org/10.5194/cp-13-1919-](https://doi.org/10.5194/cp-13-1919-2017)
812 2017

813 Shi, H., Wang, B., Cook, E.R., Liu, J., Liu, F., 2018. Asian summer precipitation over the past 544 years
814 reconstructed by merging tree rings and historical documentary records. *J. Clim.* 31, 7845–
815 7861. <https://doi.org/10.1175/JCLI-D-18-0003.1>

816 Sinha, A., Berkelhammer, M., Stott, L., Mudelsee, M., Cheng, H., Biswas, J., 2011. The leading mode of
817 Indian Summer Monsoon precipitation variability during the last millennium. *Geophys. Res.*
818 *Lett.* 38, 15. <https://doi.org/10.1029/2011GL047713>

819 Sinha, A., Kathayat, G., Cheng, H., Breitenbach, S.F.M., Berkelhammer, M., Mudelsee, M., Biswas, J.,
820 Edwards, R.L., 2015. Trends and oscillations in the Indian summer monsoon rainfall over the
821 last two millennia. *Nat. Commun.* 6. <https://doi.org/10.1038/ncomms7309>

822 Slivinski, L.C., Compo, G.P., Whitaker, J.S., Sardeshmukh, P.D., Giese, B.S., McColl, C., Allan, R., Yin, X.,
823 Vose, R., Titchner, H., Kennedy, J., Spencer, L.J., Ashcroft, L., Brönnimann, S., Brunet, M.,
824 Camuffo, D., Cornes, R., Cram, T.A., Crouthamel, R., Domínguez-Castro, F., Freeman, J.E.,
825 Gergis, J., Hawkins, E., Jones, P.D., Jourdain, S., Kaplan, A., Kubota, H., Le Blancq, F., Lee, T.,
826 Lorrey, A., Luterbacher, J., Maugeri, M., Mock, C.J., Moore, G.W.K., Przybylak, R., Pudmenzky,
827 C., Reason, C., Slonosky, V.C., Smith, C., Tinz, B., Trewin, B., Valente, M.A., Wang, X.L.,
828 Wilkinson, C., Wood, K., Wyszyn'ski, P., 2019. Towards a more reliable historical reanalysis:
829 Improvements for version 3 of the Twentieth Century Reanalysis system. *Q. J. R. Meteorol.*
830 *Soc.* qj.3598. <https://doi.org/10.1002/qj.3598>

831 Stoffel, M., Khodri, M., Corona, C., Guillet, S., Poulain, V., Bekki, S., Guiot, J., Luckman, B.,
832 Oppenheimer, C., Lebas, N., Beniston, M., Masson-Delmotte, V., 2015. Estimates of volcanic-
833 induced cooling in the Northern Hemisphere over the past 1,500 years. *Nat. Geosci.* 8, 784–
834 788. <http://dx.doi.org/10.1038/ngeo2526>

835 Sun, A., Feng, Z., 2013. Holocene climatic reconstructions from the fossil pollen record at Qigai Nuur in
836 the southern Mongolian Plateau. *Holocene* 23, 1391–1402.
837 <https://doi.org/10.1177/0959683613489581>

838 Talento, S., Schneider, L., Werner, J., Luterbacher, J., 2019. Millennium-length precipitation
839 reconstruction over south-eastern Asia: a pseudo-proxy approach. *Earth Syst. Dyn.* 10, 347–
840 364. <https://doi.org/10.5194/esd-10-347-2019>

841 Tan, L., Cai, Y., An, Z., Edwards, R.L., Cheng, H., Shen, C.-C., Zhang, H., 2010. Centennial- to decadal-
842 scale monsoon precipitation variability in the semi-humid region, northern China during the
843 last 1860 years: Records from stalagmites in Huangye Cave. *The Holocene* 21, 287–296.
844 <https://doi.org/10.1177/0959683610378880>

845 Tan, L., Yanjun Cai, Liang Yi, Zhisheng An, Li Ai, 2008. Precipitation variations of Longxi, northeast
846 margin of Tibetan Plateau since AD 960 and their relationship with solar activity. *Clim. Past* 4,
847 19–28. <https://doi.org/10.5194/cp-4-19-2008>

848 Treydte, K.S., Schleser, G.H., Helle, G., Frank, D.C., Winiger, M., Haug, G.H., Esper, J., 2006. The
849 twentieth century was the wettest period in northern Pakistan over the past millennium.
850 *Nature* 440, 1179–1182. <https://doi.org/10.1038/nature04743>

851 Wan, H., Zhang, X., Zwiers, F. W., Shiogama, H. 2013. Effect of data coverage on the estimation of mean
852 and variability of precipitation at global and regional scales. *J. Geophys. Res.* 118, 534–546.
853 <https://doi.org/10.1002/jgrd.50118>

854 Wang, J., Yang, B., Ljungqvist, F.C., Luterbacher, J., Osborn, T.J., Briffa, K.R., Zorita, E., 2017. Internal
855 and external forcing of multidecadal Atlantic climate variability over the past 1,200 years. *Nat.*
856 *Geosci.*, 10, 512–517. <https://doi.org/10.1038/NGEO2962>

857 Wang, Liang-Chi, Behling, H., Lee, T.-Q., Li, H.-C., Huh, C.-A., Shiau, L.-J., Chen, S.-H., Wu, J.-T., 2013.
858 Increased precipitation during the Little Ice Age in northern Taiwan inferred from diatoms and
859 geochemistry in a sediment core from a subalpine lake. *J. Paleolimnol.* 49, 619–631.
860 <https://doi.org/10.1007/s10933-013-9679-9>

861 Wang, Wei, Feng, Z., Ran, M., Zhang, C., 2013. Holocene climate and vegetation changes inferred from
862 pollen records of Lake Aibi, northern Xinjiang, China: A potential contribution to understanding
863 of Holocene climate pattern in East-central Asia. *Quat. Int.* 311, 54–62.
864 <https://doi.org/10.1016/j.quaint.2013.07.034>

865 Wang, W. Z., Liu, X., Xu, G., Shao, X., Qin, D., Sun, W., An, W., Zeng, X., 2013. Moisture variations over
866 the past millennium characterized by Qaidam Basin tree-ring $\delta^{18}\text{O}$. *Chin. Sci. Bull.* 58, 3956–
867 3961. <https://doi.org/10.1007/s11434-013-5913-0>

868 Wang, Y., Cheng, H., Edwards, R.L., He, Y., Kong, X., An, Z.S., Wu, J., Kelly, M.J., Dykoski, C.A., Li, X.,
869 2005. The Holocene Asian Monsoon: Links to Solar Changes and North Atlantic Climate.
870 *Science* 308, 854–857. <https://doi.org/10.1126/science.1106296>

871 Wetter, O., Pfister, C., 2011. Spring-summer temperatures reconstructed for northern Switzerland and
872 southwestern Germany from winter rye harvest dates, 1454–1970. *Clim. Past* 7, 1307–1326.
873 <https://doi.org/10.5194/cp-7-1307-2011>

874 Wigley, T.M., Briffa, K.R., Jones, P.D., 1984. On the average value of correlated time series, with
875 applications in dendroclimatology and hydrometeorology. *J. Clim. Appl. Meteorol.* 23, 201–
876 213.

877 Wilson, R., Anchukaitis, K.J., Briffa, K., Büntgen, U., Cook, E.R., D'Arrigo, R.D., Davi, N., Esper, J., Frank,
878 D., Gunnarson, B., Hegerl, G., Klesse, S., Krusic, P.J., Linderholm, H., Myglan, V., Peng, Z.,
879 Rydval, M., Schneider, L., Schurer, A., Wiles, G., and Zorita, E., 2016. Last millennium northern
880 hemisphere summer temperatures from tree rings: Part I: The long term context. *Quat. Sci.*
881 *Rev.* 134, 1–18.

882 Xiao, J., Si, B., Zhai, D., Itoh, S., Lomtadze, Z., 2008. Hydrology of Dali Lake in central-eastern Inner
883 Mongolia and Holocene East Asian monsoon variability. *J. Paleolimnol.* 40, 519–528.
884 <https://doi.org/10.1007/s10933-007-9179-x>

885 Xing, P., Chen, X., Luo, Y., Nie, S., Zhao, Z., Huang, J., Wang, S., 2016. The Extratropical Northern
886 Hemisphere Temperature Reconstruction during the Last Millennium Based on a Novel
887 Method. *PLOS ONE* 11, e0146776. <https://doi.org/10.1371/journal.pone.0146776>

888 Xoplaki, E., Luterbacher, J., Paeth, H., Dietrich, D., Steiner N., Grosjean, M., Wanner, H., 2005. European
889 spring and autumn temperature variability and change of extremes over the last half
890 millennium. *Geophys. Res. Lett.* 32: L15713. <https://doi.org/10.1029/2005GL023424>

891 Xoplaki, E., Fleitmann, D., Luterbacher, J., Wagner, S., Haldon, J.F., Zorita, E., Telelis, I., Toreti, A.,
892 Izdebski, A., 2016. The Medieval Climate Anomaly and Byzantium: A review of the evidence on
893 climatic fluctuations, economic performance and societal change. *Quat. Sci. Rev.* 136, 229–
894 252. <https://doi.org/10.1016/j.quascirev.2015.10.004>

895 Xoplaki, E., Luterbacher, J., Wagner, S., Zorita, E., Fleitmann, D., Preiser-Kapeller, J., Sargent, A.M.,
896 White, S., Toreti, A., Haldon, J.F., Mordechai, L., Bozkurt, D., Akçer-Ön, S., Izdebski, A., 2018.
897 Modelling Climate and Societal Resilience in the Eastern Mediterranean in the Last Millennium.
898 *Hum. Ecol.* 46, 363–379. <https://doi.org/10.1007/s10745-018-9995-9>

899 Yan, Z., Li, Z., Wang, X., 1993. An analysis of decade to century scale climatic jumps in history. *Chin. J.*
900 *Atmospheric Sci.* 17, 663–671.

901 Yang, B., Qin, C., Shi, F., Sonechkin, D.M., 2012. Tree ring-based annual streamflow reconstruction for
902 the Heihe River in arid northwestern China from AD 575 and its implications for water resource
903 management. *The Holocene* 22, 773–784. <https://doi.org/10.1177/0959683611430411>

904 Yang, B., Kang, S., Ljungqvist, F.C., He, M., Zhao, Y., Qin, C., 2014a. Drought variability at the northern
905 fringe of the Asian summer monsoon region over the past millennia. *Clim. Dyn.* 43, 845–859.
906 <https://doi.org/10.1007/s00382-013-1962-y>

907 Yang, B., Qin, C., Wang, J., He, M., Melvin, T.M., Osborn, T.J., Briffa, K.R., 2014b. A 3,500-year tree-ring
908 record of annual precipitation on the northeastern Tibetan Plateau. *Proc. Natl. Acad. Sci.* 111,
909 2903–2908. <https://doi.org/10.1073/pnas.1319238111>

910 Yao, T., Thompson, L., Qin, D., Tian, L., 1996. Variations in temperature and precipitation in the past 2
911 000 a on the Xizang (Tibet) Plateau–Guliya ice core record. *Sci. China Ser. D.* 4, 425–433.
912 <https://doi.org/10.1360/ym1996-39-4-425>

913 Yin, Z.-Y., Shao, X., Qin, N., Liang, E., 2007. Reconstruction of a 1436-year soil moisture and vegetation
914 water use history based on tree-ring widths from Qilian junipers in northeastern Qaidam Basin,
915 northwestern China. *Int. J. Climatol.* 28, 37–53. <https://doi.org/10.1002/joc.1515>

916 Yu, X., Zhou, W., Franzen, L.G., Xian, F., Cheng, P., Jull, A.J.T., 2006. High-resolution peat records for
917 Holocene monsoon history in the eastern Tibetan Plateau. *Sci. China Ser. D* 49, 615–621.
918 <https://doi.org/10.1007/s11430-006-0615-y>

919 Zhang, H., Werner, J.P., García-Bustamante, E., González-Rouco, F., Wagner, S., Zorita, E., Fraedrich,
920 K., Jungclaus, J.H., Ljungqvist, F.C., Zhu, X., Xoplaki, E., Chen, F., Duan, J., Ge, Q., Hao, Z., Ivanov,
921 M., Schneider, L., Talento, S., Wang, J., Yang, B., Luterbacher, J., 2018. East Asian warm season
922 temperature variations over the past two millennia. *Sci. Rep.* 8: 7702.n
923 <https://doi.org/10.1038/s41598-018-26038-8>

924 Zeng, Y., Chen, J., Zhu, Z., Li, J., Wang, J., Wan, G., 2012. The wet Little Ice Age recorded by sediments
925 in Huguangyan Lake, tropical South China. *Quat. Int.* 263, 55–62.
926 <https://doi.org/10.1016/j.quaint.2011.12.022>

927 Zhai, D., Xiao, J., Zhou, L., Wen, R., Chang, Z., Wang, X., Jin, X., Pang, Q., Itoh, S., 2011. Holocene East
928 Asian monsoon variation inferred from species assemblage and shell chemistry of the
929 ostracodes from Hulun Lake, Inner Mongolia. *Quat. Res.* 75, 512–522.
930 <https://doi.org/10.1016/j.yqres.2011.02.008>

931 Zhang, P., Cheng, H., Edwards, R.L., Chen, F., Wang, Y., Yang, X., Liu, J., Tan, M., Wang, X., Liu, J., An, C.,
932 Dai, Z., Zhou, J., Zhang, D., Jia, J., Jin, L., Johnson, K.R., 2008. A Test of Climate, Sun, and Culture
933 Relationships from an 1810-Year Chinese Cave Record. *Science* 322, 940–942.
934 <https://doi.org/10.1126/science.1163965>

935 Zhang, Q., Gemmer, M., Chen, J., 2008. Climate changes and flood/drought risk in the Yangtze Delta,
936 China, during the past millennium. *Quat. Int.* 176–177, 62–69.
937 <https://doi.org/10.1016/j.quaint.2006.11.004>

938 Zhang, Y., Tian, Q., Gou, X., Chen, F., Leavitt, S.W., Wang, Y., 2011. Annual precipitation reconstruction
939 since AD 775 based on tree rings from the Qilian Mountains, northwestern China. *Int. J.*
940 *Climatol.* 31, 371–381. <https://doi.org/10.1002/joc.2085>

941 Zhang, H., Yuan, N., Esper, J., Werner, J.P., Xoplaki, E., Büntgen, U., Treydte, K., Luterbacher, J., 2015.
942 Modified climate with long term memory in tree ring proxies. *Environ. Res. Lett.* 10, 084020.
943 <https://doi.org/10.1088/1748-9326/10/8/084020>

944 Zhang, H., Werner, J.P., García-Bustamante, E., González-Rouco, F., Wagner, S., Zorita, E., Fraedrich,
945 K., Jungclaus, J.H., Ljungqvist, F.C., Zhu, X., Xoplaki, E., Chen, F., Duan, J., Ge, Q., Hao, Z., Ivanov,
946 M., Schneider, L., Talento, S., Wang, J., Yang, B., Luterbacher, J., 2018. East Asian warm season
947 temperature variations over the past two millennia. *Sci. Rep.* 8.
948 <https://doi.org/10.1038/s41598-018-26038-8>

949 Zheng, J., Wang, W.-C., Ge, Q., Man, Z., Zhang, P., 2006. Precipitation Variability and Extreme Events
950 in Eastern China during the Past 1500 Years. *Terr. Atmospheric Ocean. Sci.* 17, 579.
951 [https://doi.org/10.3319/TAO.2006.17.3.579\(A\)](https://doi.org/10.3319/TAO.2006.17.3.579(A))

952 Zhou, A., Sun, H., Chen, F., Zhao, Y., An, C., Dong, G., Wang, Z., Chen, J., 2010. High-resolution climate
953 change in mid-late Holocene on Tianchi Lake, Liupan Mountain in the Loess Plateau in central
954 China and its significance. *Chin. Sci. Bull.* 55, 2118–2121. [https://doi.org/10.1007/s11434-010-](https://doi.org/10.1007/s11434-010-3226-0)
955 [3226-0](https://doi.org/10.1007/s11434-010-3226-0)

956

Table and figure captions

957 Table 1: Millennial long proxy records for hydroclimate investigations in Monsoon Asia. Site numbers as in Fig. 1.
958 Abbreviations: Lon=Longitude, Lat=Latitude, DA=Dating accuracy, EC=Evidence for climate signal, TRE= Tree-rings, LAK=Lake
959 sediments, POL=Pollen, SPE=Speleothems, ICE=Ice-cores, DOC=Documentary, ISO=Tree-ring isotopes, TRW= Tree-ring width,
960 TOC=Total organic carbon.

961 Table 2: EPS-values for the subregions as defined in Fig. 1.

962 Figure 1: Millennial-long proxy network for hydroclimate investigations in Monsoon Asia covering the area 70°-130°E and 20°-
963 50°N. The three regions indicated by dashed circles are used for spatial data aggregation (NE Tibetan Plateau=Northeastern
964 Tibetan Plateau; NC China= Northcentral China; SE China= Southeastern China; see section “Effects of proxy selection based
965 on the suitability assessment”). See Table 1 for details on the proxies.

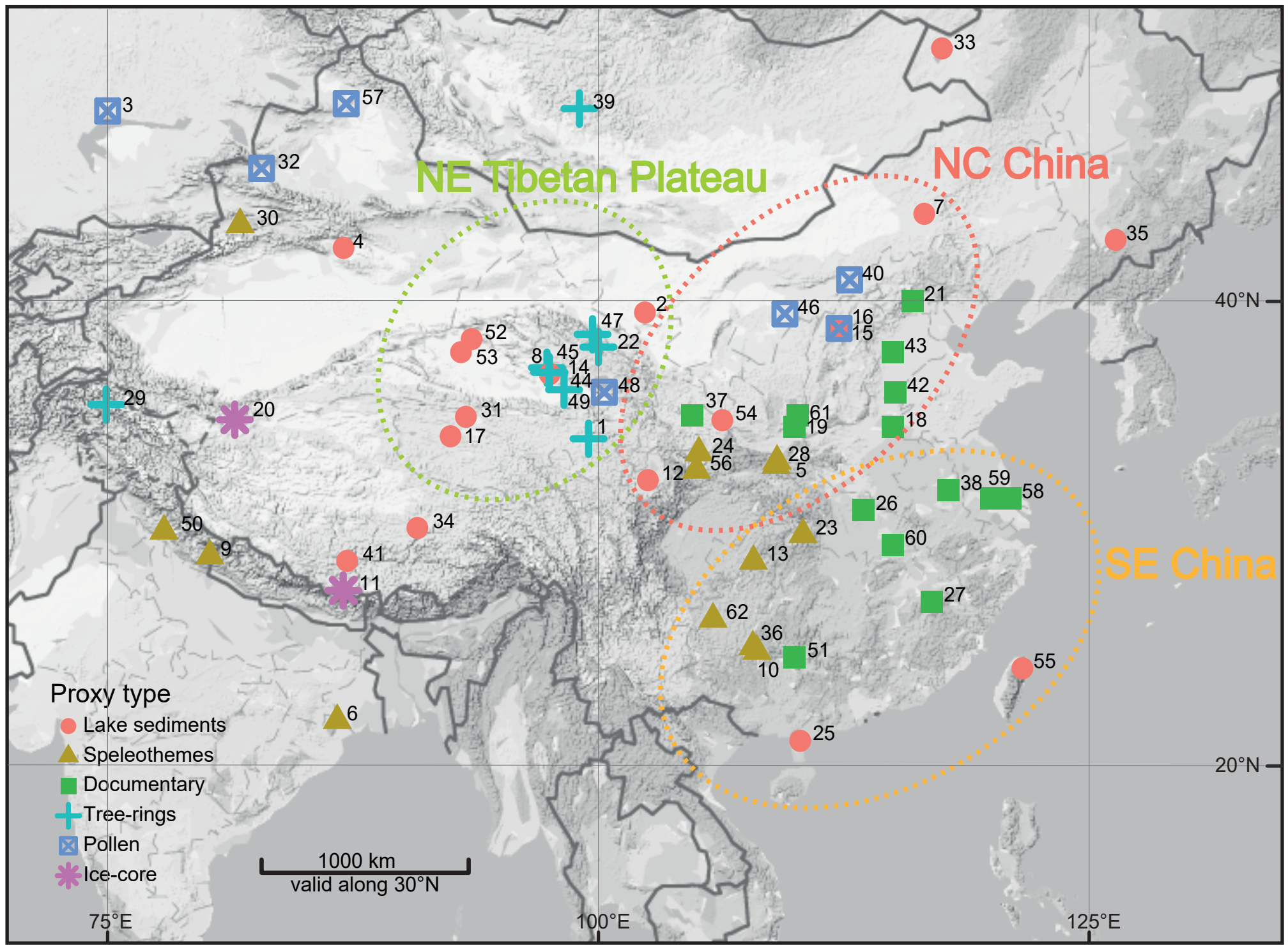
966 Figure 2: Spearman correlation of proxy records with the gridded precipitation field of Shi17 for the period 1470-1950 CE. (a)
967 Low-pass filtered data, colors indicate DA class. (b) Low-pass filtered data, colors indicate EC class. (c) Band-pass filtered data,
968 colors indicate DA class. (d) Band-pass filtered data, colors indicate EC class. Dashed lines indicate the $p=0.1$ significance
969 threshold. Records marked with grey bars are not fully independent from Shi17. The independence of three studies (in
970 Chinese) could not be evaluated (question marks below the top margin). The records are indicated by their number (Table 1)
971 and ordered into groups: LAK=Lake sediments, SPE=Speleothems, POL=Pollen, ICE=Ice-cores, ISO=Tree-ring isotopes, TRE=
972 Tree-rings, DOC=Documentary.

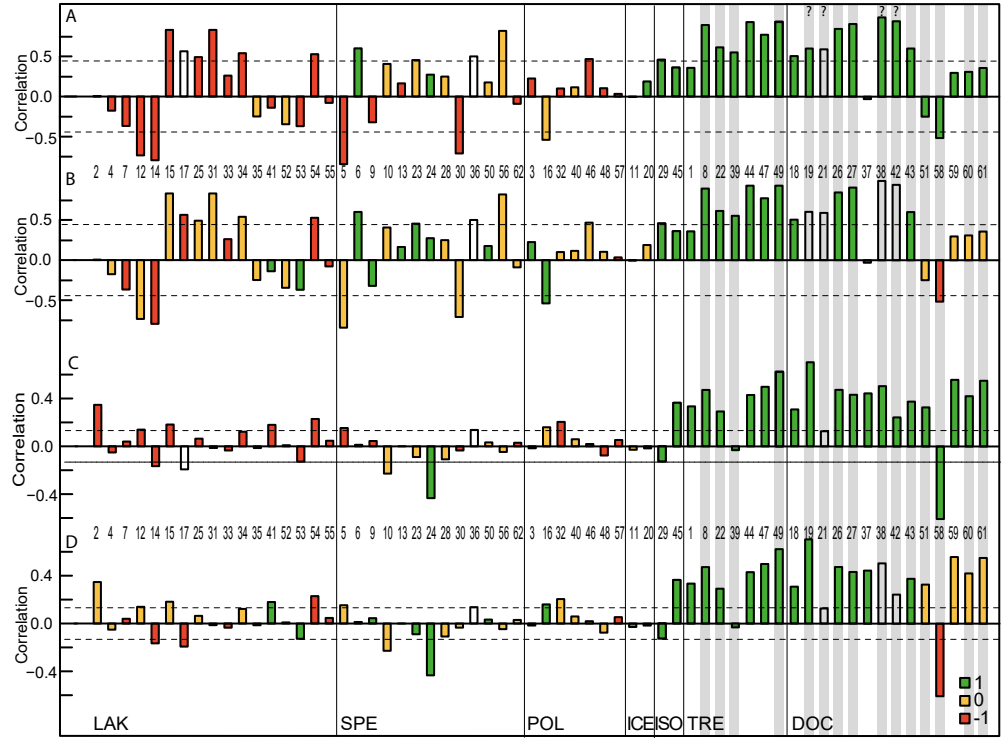
973 Figure 3: Correlation of proxy records with a mean of their six closest neighbors plotted against the mean distance of the
974 neighbors. (a) The correlation is calculated with low-pass filtered data for the period 1100-1900 CE. Colors refer to DA
975 classification. (b) Same as (a), but colors refer to EC. (c) Same as (a), but for band-pass filtered data. (d) Same as (c), but colors
976 refer to EC. Symbols indicate the type of proxy being tested, not the type of their neighbors. Dotted and dashed lines refer to
977 the 95% and 90% significance levels. Records 29 and 44 are tree-ring isotope records.

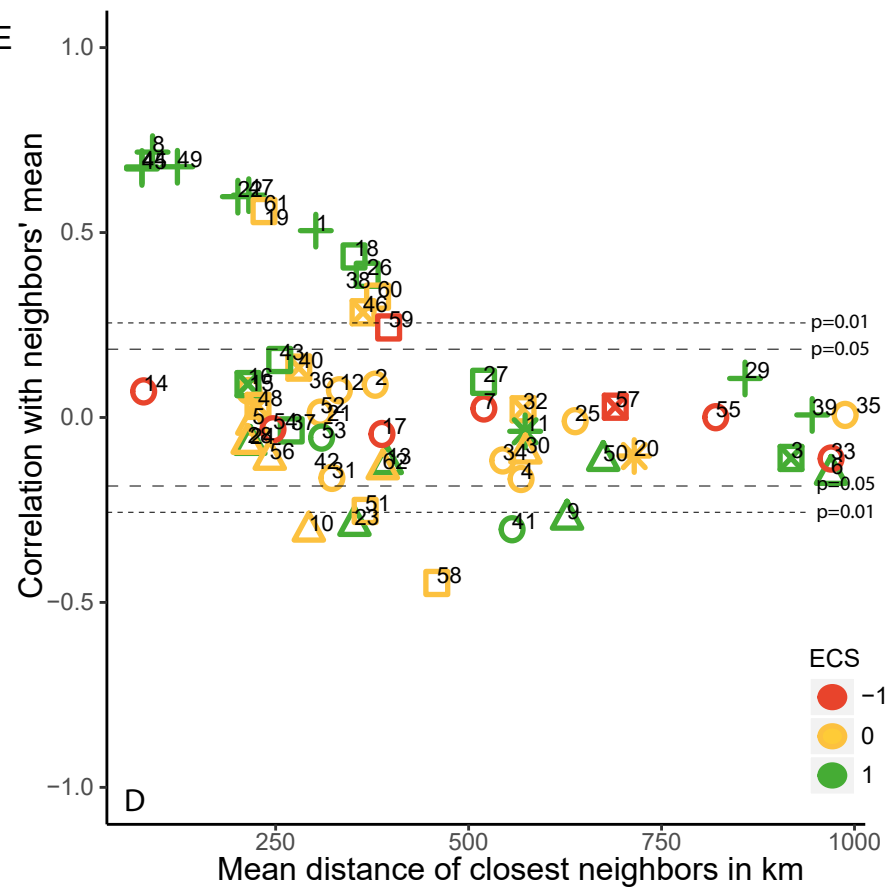
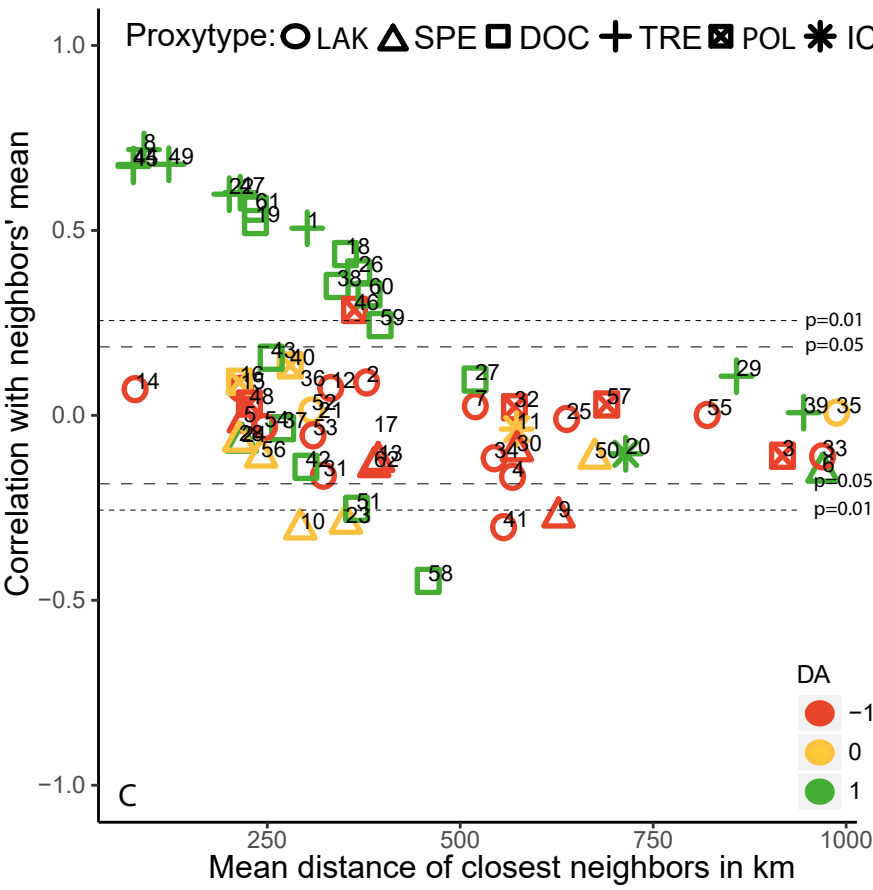
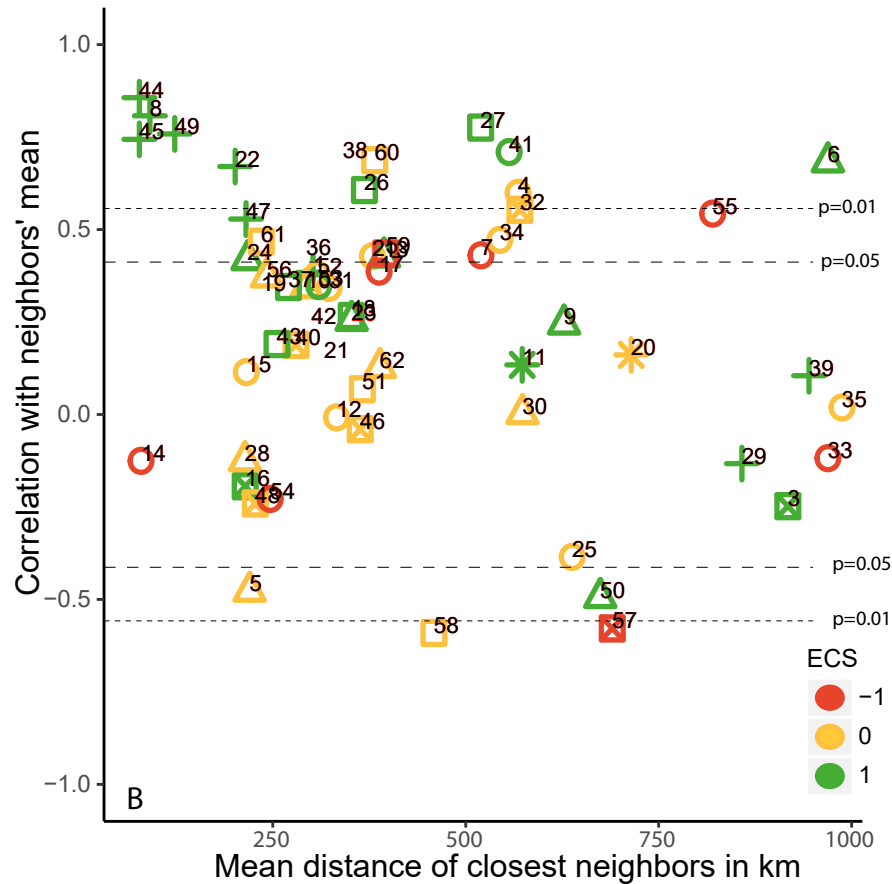
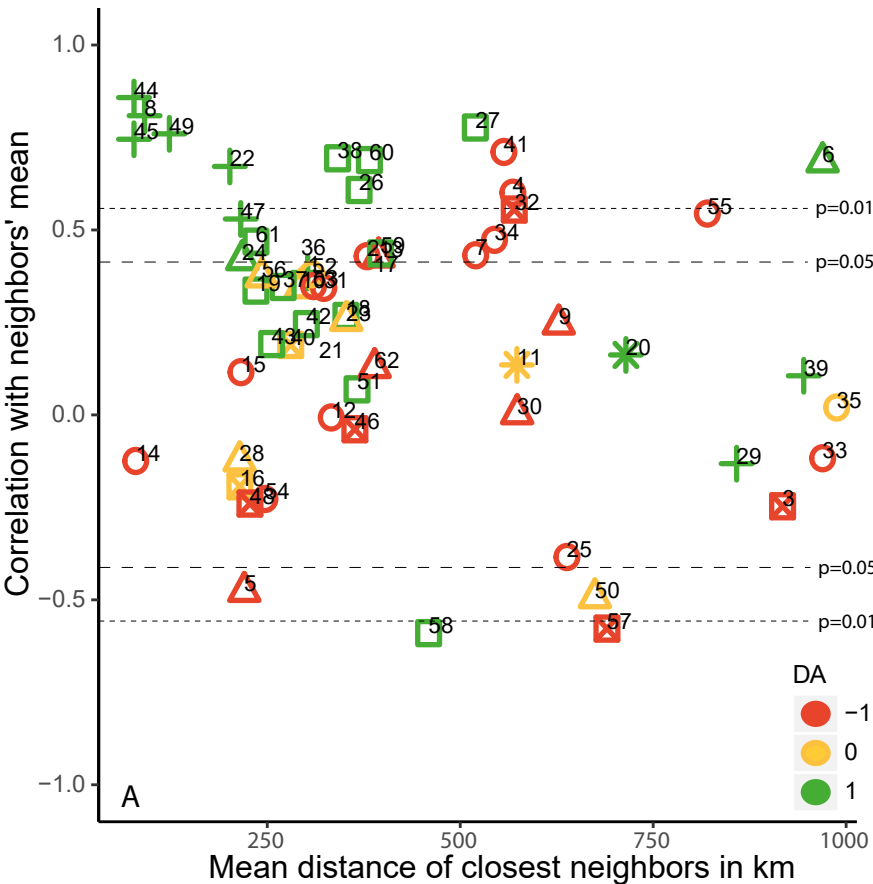
978 Figure 4: Autocorrelation at lag 10 and 50 year, respectively, of the filtered and resampled proxy records for the period 1000-
979 1900 CE. Left (right) bars indicate the autocorrelation for low(band)-pass filtered time-series. (a) Grouped by proxy type. (b)
980 Grouped by DA. (c) Grouped by EC. TRE includes the isotope records.

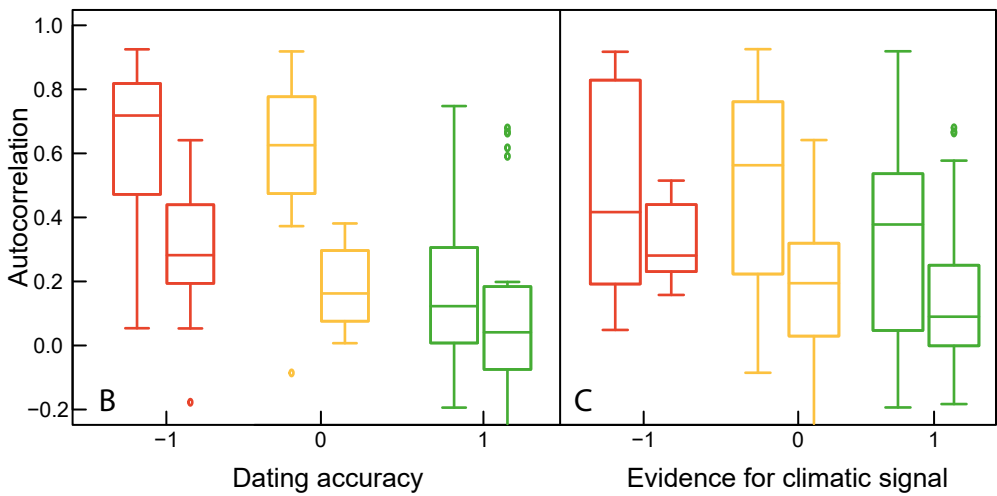
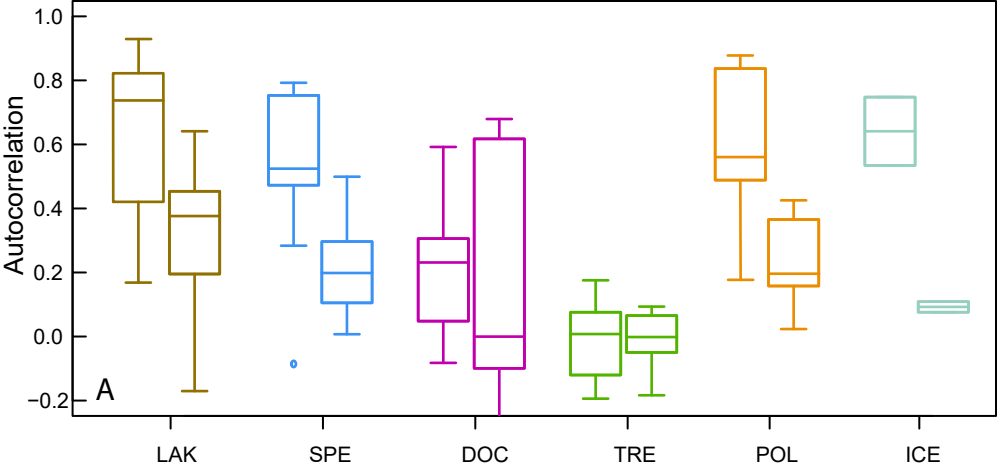
981 Figure 5: Spatial aggregation of Monsoon Asian proxy records, after smoothing and resampling with 50-years resolution to
982 account for irregular time-steps in the original records. (A) Northeastern Tibetan Plateau proxy records averaged by archive
983 type, (B) Northeastern Tibetan Plateau proxy records averaged by suitability classification, (C) Northcentral China proxy
984 records averaged by archive type, (D) Northcentral China proxy records averaged by suitability classification, (E) Southeastern
985 China proxy records averaged by archive type, (F) Southeastern China proxy records averaged by suitability classification.

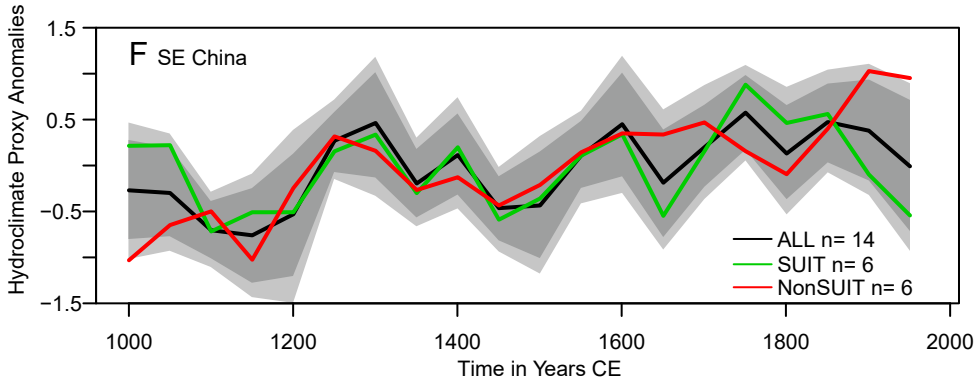
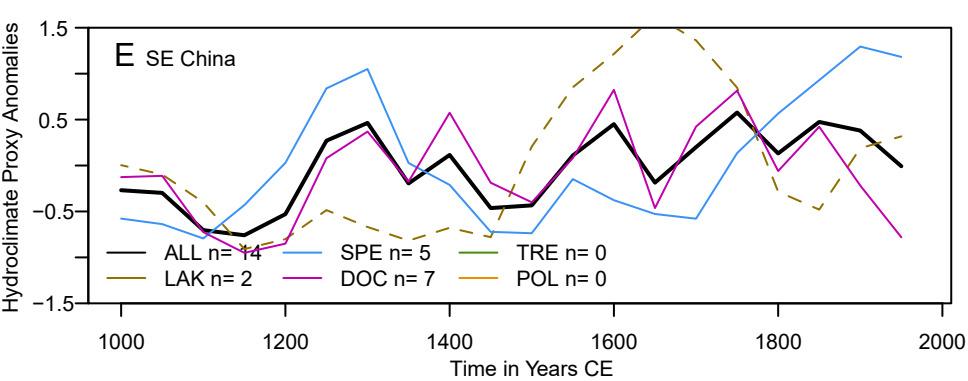
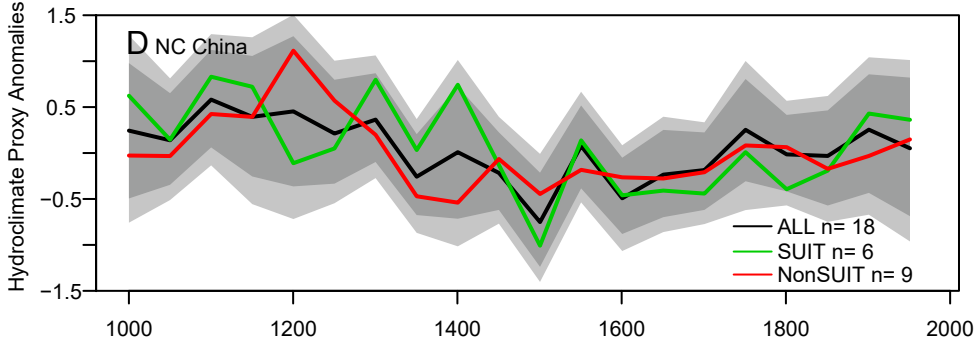
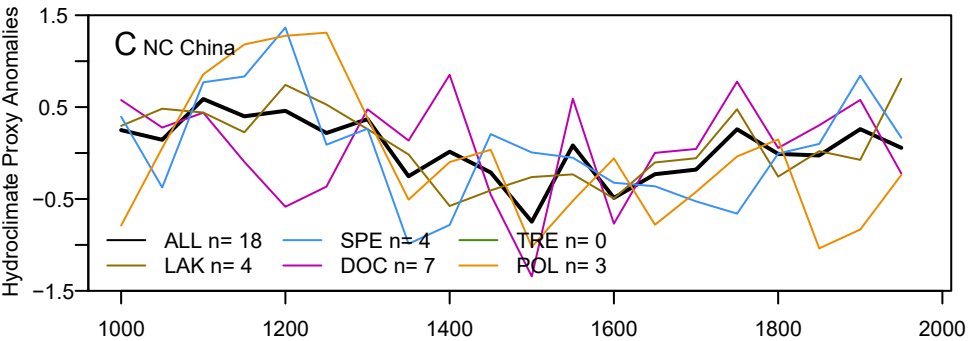
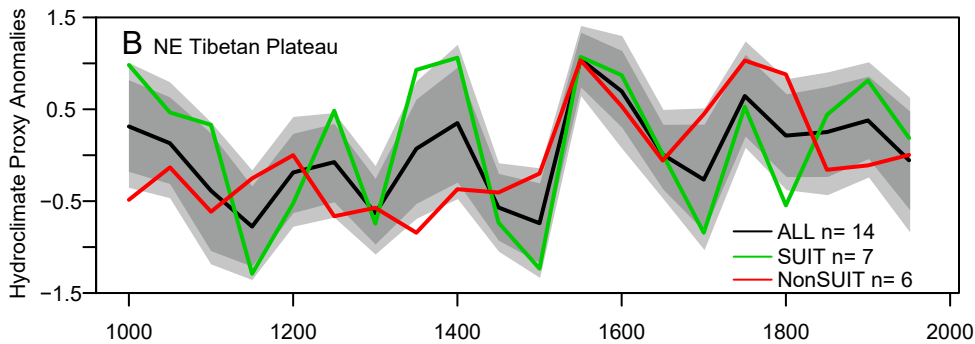
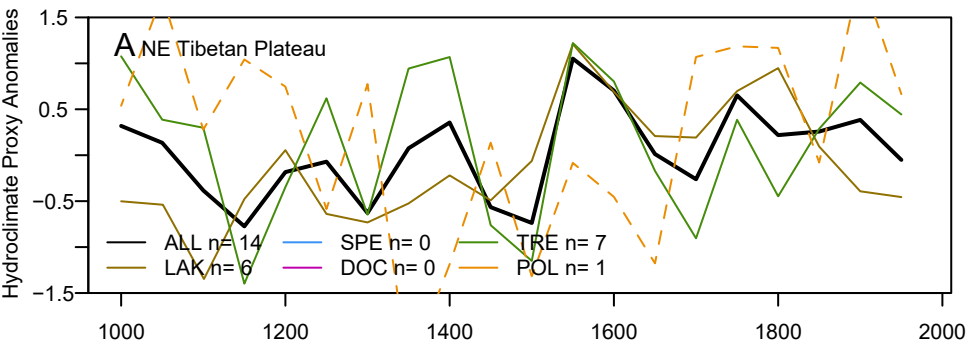
986 Shaded areas in (B), (D) and (F) represent the results of a bootstrapping experiment for a reduced average using a subsampling
987 over all proxy-records in each region (5th and 95th percentile: dark grey; 1st and 99th percentile: light grey). Records are only
988 shown until 1950 because many datasets terminate in the late 20th century. All proxy records are standardized over the
989 common period 1000-1900 CE. Dashed lines in the left-hand column indicates an archive size <3.











Nr	Site	Sub-region	Lon	Lat	Archive	Proxy type	Start (Years CE)	End (Years CE)	Resolution (Years)	DA	EC	References
1	Anyemaqen Mountains	1	99.5	34.5	TRE	TRW	800	2004	1	1	1	Gou et al., 2010
2	Badain Jaran Desert	1	102.4	39.55	LAK	Chloride	815	1983	6	-1	0	Ma and Edmunds, 2006
3	Balkhash Basin		75	46.9	POL	Pollen	785	1950	11	-1	1	Feng et al., 2013
4	Bosten Lake ^a		87.0	42	LAK	Var. ^a	-39	2000	11	-1	0	Chen et al., 2006
5	Buddha Cave	2	109.1	33.4	SPE	$\delta^{18}\text{O}$	800	1996	2	-1	0	Paulsen et al., 2003
6	Central India composite ^b		86.7	22.1	SPE	$\delta^{18}\text{O}$	625	2007	1	1	1	Sinha et al., 2011
7	Dali Lake	2	116.6	43.26	LAK	TOC	-9	1921	27	-1	-1	Xiao et al., 2008
8	Delingha	1	97.4	37.38	TRE	TRW	-499	2011	1	1	1	Yang et al., 2014a
9	Dharamjali Cave		80.2	29.52	SPE	$\delta^{18}\text{O}$	794	1991	10	-1	1	Sanwal et al., 2013
10	Dongge Cave	3	108.1	25.28	SPE	$\delta^{18}\text{O}$	3	2000	4	0	0	Wang et al., 2005
11	East Rongbuk		87	28	ICE	dD	1000	1990	6	0	1	Kaspari et al., 2007
12	Eastern Tibetan Plateau	2	102.5	32.77	LAK	Humification	754	1900	76	-1	0	Yu et al., 2006
13	Furong Cave	3	107.9	29.29	SPE	$\delta^{18}\text{O}$	2	2005	7	-1	1	Li et al., 2011
14	Gahai Lake	1	97.5	37.13	LAK	%C37:4	-1	1962	5	-1	-1	He et al., 2013
15	Gonghai Lake	2	112.2	38.87	LAK	S-300 ^d	842	2000	5	-1	0	Liu et al., 2011
16	Gonghai Pollen	2	112.3	38.93	POL	Pollen	-10	2008	20	0	1	Chen et al., 2015a
17	Goulucuo Lake	1	92.5	34.6	LAK	CaCO ₃ %	964	1992	11	?	-1	Li et al., 2004
18	Great Bend Yellow River	2	115	35	DOC	Documentary	804	1945	8	1	1	Gong and Hameed, 1991
19	Guanzhong Plain	2	110	35	DOC	Documentary	960	2010	1	1	?	Hao et al., 2017
20	Guliya		81.5	35.28	ICE	Glacial acc.	1000	1990	10	1	0	Yao et al., 1996
21	Haihe River Basin	2	116	40	DOC	Documentary	791	1976	12	?	?	Yan et al., 1993
22	Heihe River Basin	1	100	38.2	TRE	TRW	575	2008	1	1	1	Yang et al., 2012
23	Heshang_Cave	3	110.4	30.45	SPE	$\delta^{18}\text{O}$	0	2002	3	0	1	Hu et al., 2008
24	Huangye Cave	2	105.1	33.92	SPE	$\delta^{18}\text{O}$	138	2002	4	1	1	Tan et al., 2010
25	Huguangyan Lake	3	110.3	21.15	LAK	TOC	780	2004	12	-1	0	Zeng et al., 2012

26	Jianghuai	3	113.5	31.5	DOC	Documentary	773	1990	22	1	1	Zheng et al., 2006
27	Jiangnan	3	117	27.5	DOC	Documentary	776	1992	19	1	1	Zheng et al., 2006
28	Jiuxian Cave	2	109.1	33.57	SPE	$\delta^{18}\text{O}$	0	1998	4	0	0	Cai et al., 2010
29	Karakorum Mountains		74.9	35.9	TRE ^c	$\delta^{18}\text{O}$	1000	1998	1	1	1	Treydte et al., 2006
30	Kesang Cave		81.8	42.87	SPE	$\delta^{18}\text{O}$	14	1945	21	-1	0	Cheng et al., 2012
31	Kusai Lake	1	93.25	35.4	LAK	TOC	8	2006	13	-1	0	Liu et al., 2009
32	Lake Aibi		82.84	44.9	POL	A/C ratio	-21	1950	16	-1	0	Wang et al., 2013
33	Lake Hulun		117.5	49	LAK	$\delta^{18}\text{O}$	5	1955	38	-1	-1	Zhai et al., 2011
34	Lake Nam Co		90.8	30.73	LAK	Mineralogy	3	2007	5	-1	0	Kasper et al., 2012
35	Lake Xiaolongwan		126.4	42.3	LAK	$\delta^{13}\text{C}$	797	2002	14	0	0	Chu et al., 2009
36	Longquan Cave	3	107.9	25.48	SPE	$\delta^{18}\text{O}$	981	1911	7	?	?	Qin et al., 2008
37	Longxi area	2	104.8	35.45	DOC	Documentary	960	1990	11	1	1	Tan et al., 2008
38	Lower Huai River	3	117.8	32.36	DOC	Documentary	-5	1955	10	1	?	Man, 2009
39	Mongolia		99	47	TRE	TRW	900	2011	1	1	1	Pederson et al., 2014
40	Monsoonal Northern China	2	112.8	40.8	POL	Pollen	-202	2003	3	0	0	Li et al., 2017b
41	Ngamring Tso		87.2	29.3	LAK	Grainsize PC1	-70	2005	23	-1	1	Conroy et al., 2017
42	North China	2	115.1	36.4	DOC	Documentary	-5	1945	10	1	?	Man, 2009
43	North China Plains	2	115	38	DOC	Documentary	777	1990	28	1	1	Zheng et al., 2006
44	Qaidam Basin	1	97.5	37.2	TRE ^c	$\delta^{18}\text{O}$	998	2009	3	1	1	Wang et al., 2013
45	Qaidam Basin	1	97.5	37.2	TRE	TRW	566	2002	1	1	1	Yin et al., 2007
46	Qigai Nuur	2	109.5	39.5	POL	Pollen	784	1932	16	-1	0	Sun and Feng, 2013
47	Qilian Mountains	1	99.5	38.5	TRE	TRW	800	1950	1	1	1	Zhang et al., 2011
48	Qinghai Dalianhai	1	100.3	36.44	POL	Pollen	0	1994	24	-1	0	Li et al., 2017a
49	Qinghai Province	1	99	37	TRE	TRW	157	1993	1	1	1	Sheppard et al., 2004
50	Sahiya Cave		77.9	30.6	SPE	$\delta^{18}\text{O}$	-141	2006	1	0	1	Sinha et al., 2015

51	Southern China	3	110	25	DOC	Documenta ry	953	1996	5	1	0	Qian et al., 2003
52	Sugan Lake	1	93.9	38.5	LAK	Salinity	990	2002	11	0	0	Chen et al., 2009
53	Sugan Lake	1	93.9	38.85	LAK	%C37:4	794	2006	12	-1	1	He et al., 2013
54	Tianchi Lake	2	106.3	35.26	LAK	Redness	0	1995	5	-1	-1	Zhou et al., 2010
55	Tsuifong Lake	3	121.6	24.5	LAK	Diatoms	792	2006	12	-1	-1	Wang et al., 2013
56	Wanxiang Cave	2	105	33.19	SPE	$\delta^{18}\text{O}$	192	2003	3	0	0	Zhang et al., 2008
57	Wulungu Lake		87.15	47.15	POL	Pollen	56	1927	36	-1	-1	Liu et al., 2008
58	Yangtze Delta	3	120	32	DOC	Documenta ry	1000	2000	9	1	0	Jiang et al., 2005
59	Yangtze Delta	3	121	32	DOC	Documenta ry	1000	2000	5	1	-1	Zhang et al., 2008
60	Yangtze River	3	115	30	DOC	Documenta ry	942	1996	4	1	0	Qian et al., 2003
61	Yellow River	2	110	35	DOC	Documenta ry	950	1999	1	1	0	Qian et al., 2003
62	Zhijin Cave	3	105.8	26.73	SPE	$\delta^{18}\text{O}$	884	2004	2	-1	0	Kuo et al., 2011

^a Chen et al. (2006) analyze carbon content, grain size and pollen for reconstructing the hydroclimate past of Bosten Lake. We use an average of the three indices $\text{CaCO}_3\%$ (inverted), mean grain size and pollen A/C ratio after linear interpolation between the time steps which vary among the three time-series.

^bThe Central India Composite is based on two stalagmites from spatially separated caves. The coordinates here represent an average of the two locations.

^cTree-ring isotope records.

^d S_{300} is a proxy for magnetic mineral concentrations.

Region	SE/SD-ratio	
	Full average	Subset average
NE Tibetan Plateau	0.76	0.89
NC China	0.51	0.33
SE China	0.60	0.21
